

AUTOREFERAT (English version)

1. Personal data

- Name, surname: Janusz Edward Jacak
- Date and place of birth: 9.01.1983, Wrocław
- Employed by: Wrocław University of Science and Technology, Faculty of Fundamental Problems of Technology

2. Degrees

- MSc Eng. in Physics, Faculty of Fundamental Problems of Technology, Wrocław University of Science and Technology, 2007
- MSc Eng. in Computer Science, Faculty of Computer Science, Wrocław University of Science and Technology, 2007
- PhD in Physics, Faculty of Fundamental Problems of Technology, Wrocław University of Science and Technology, 2011, Thesis title: "Application of braid groups in physics of 2D Hall systems (explanation of composite fermion structure)"

3. Employment track

- 2007 – 2011 PhD student in Institute of Physics, Wrocław University of Science and Technology
- 2011 – 2013 Assistant in Institute of Physics, Wrocław University of Science and Technology
- 2013 – Assistant Professor in Institute of Physics, Wrocław University of Science Technology, since 2014 in Department of Quantum Technologies, Faculty of Fundamental Problems of Technology, Wrocław University of Science and Technology (after closure and reorganization of Institute of Physics at WUST)

4. Indication of the scientific achievement

a) The title of the achievement:

Topological quantum effects in multiply connected 2D spaces and applications to Hall physics in 2DEG GaAs and in graphene monolayer and bilayer"

b) List of publications included to the habilitation dissertation:

1. **J. Jacak**, 2018, *Application of the path integral quantization to indistinguishable particle systems topologically confined by a magnetic field*, Physical Review **A 97**, 012108-1-11.
2. **J. Jacak**, 2017, *Unconventional fractional quantum Hall effect in bilayer graphene*, Scientific Reports **7**, 8720-1-13 (+ Supplementary Information 1-14).
3. **J. Jacak**, 2018, *Superfluidity of indirect excitons vs quantum Hall correlation in double Hall systems: different types of physical mechanisms of correlation organization in Hall bilayers*, Physics Letters **A**, doi.org/10.1016/j.physleta.2018.07.007.

4. **J. Jacak**, 2018, *Phase diagrams for superfluidity of indirect excitons in double Hall systems GaAs/GaAlAs/GaAs and bilayer-graphene/hBN/bilayer-graphene*, Europhysics Letters, Europhysics Letters **123**(1), 16001-1-7 (+ Supplementary Materials 1-11) doi.10.1209/0295-5075/123/16001.
5. P. Łydźba, L. Jacak, **J. Jacak**, 2015, *Hierarchy of fillings for the FQHE in monolayer graphene*, Scientific Reports **5**, 14287-1-16.
6. **J. Jacak**, L. Jacak, 2016, *Unconventional FQHE in monolayer and in bilayer graphene*, Science and Technology of Advanced Materials **17**, 149-165.
7. **J. Jacak**, L. Jacak, 2016, *Explanation of $\nu = -\frac{1}{2}$ fractional quantum Hall state in bilayer graphene*, Proceedings of the Royal Society **A 472**, 20150330-1-13.
8. **J. Jacak**, L. Jacak, 2015, *The commensurability condition and fractional quantum Hall effect hierarchy in higher Landau levels*, Pis'ma v ZhETF **102**, 23-29 (JETP Letters **102**, 19-25).
9. **J. Jacak**, L. Jacak, 2015, *Difference in hierarchy of FQHE between monolayer and bilayer graphene*, Physics Letters **A 379**, 2130-2134.
10. **J. Jacak**, L. Jacak, 2013, *On triggering role of carrier mobility for Laughlin state organization*, Pis'ma v ZhETF **98**, 776-781 (JETP Letters **98**, 684-688).
11. P. Łydźba, **J. Jacak**, 2018, *Identifying particle correlations in quantum Hall regime*, Annalen der Physik **530**, 1700221-1-19.
12. P. Łydźba, **J. Jacak**, 2017, *Topological origin and not purely antisymmetric wave functions of many-body states in the lowest Landau level*, Proceedings of the Royal Society **A 473**, 20160758-1-13.
13. **J. Jacak**, P. Łydźba, L. Jacak, 2017, *Topological approach to quantum Hall effects and its important applications: higher Landau levels, graphene and its bilayer*, European Physical Journal **B 90**, 90-1-20.
14. **J. Jacak**, L. Jacak, 2016, *Commensurability condition and hierarchy of fillings for FQHE in higher Landau levels in conventional 2DEG systems and in graphene—monolayer and bilayer*, Physica Scripta **B 90**, 015802-1-13.
15. **J. Jacak**, R. Gonczarek, L. Jacak, I. Jóźwiak, 2012, *Application of Braid Groups in 2D Hall System Physics: Composite Fermion Structure*, ISBN: 978-981-4412-02-5, World Scientific, Singapore, monograph, 1-160.

c) Description of the results:

1 Synopsis – the basic idea

The achievement concerns a novel formulation of the topological description of quantum correlations in planar electron systems exposed to a perpendicular strong magnetic field. An appropriate generalization of the Feynman path integral and introduction of the cyclotron braid group formalism allowed construction of a topological theory for FQHE¹ which occurred to be consistent with experiments and provided explanation of some aspect of former phenomenological models of FQHE and their constraints.

¹FQHE – fractional quantum Hall effect, IQHE – integral quantum Hall effect

The fundamental results for the theory developed in the framework of the presented scientific achievement is an original discovery that the quantum of magnetic field flux depends on trajectory homotopy in the case of multiply connected² space 2D with topology modified by external magnetic field. This exact result has been obtained by the author by a generalization of the Bohr-Sommerfeld rule onto a multiply connected space. This rule applied to x and y components of the kinematic momentum in 2D at presence of the perpendicular magnetic field allows for the determination of the flux quantum of this field, i.e., of the minimal size of the cyclotron orbit. The kinematic momentum components, $\hat{P}_x = -i\hbar\frac{\partial}{\partial x}$ i $\hat{P}_y = -i\hbar\frac{\partial}{\partial y} - eBx$ (at Landau gauge) create the pair of canonically conjugated variables and application to them of the Bohr-Sommerfeld rule leads to the definition of B field flux quantum, $\Phi_k = (2k + 1)\frac{h}{e}$, where k is the number of loops in a braid (or $2k + 1$ is the number of loops of multi-loop cyclotron orbit) in the multiply connected configuration space of multi-electron system on a plane, and only for $k = 0$, $\Phi_0 = \frac{h}{e}$. Multi-loop braids are elements of the full braid group B_N for the configuration space of N electrons on a plane³. The group B_N is generated by generators σ_i – exchanges of neighboring particles, i -th with $(i + 1)$ -th ones. Thus, in this group there are present the multi-loop elements (braids), σ_i^{2k+1} , $k = 1, \dots$, which are also exchanges of neighboring particles but with k additional loops. Upon the perpendicular magnetic field all braids must be built of half-parts of cyclotron trajectories. Hence, these braids have a finite size because in 2D cyclotron orbits are of finite-size defined by the magnetic field flux quantum (in contrary to 3D where a helical movement of charge along the magnetic field direction has an arbitrary long range). The braids σ_i have a range of the cyclotron orbit Φ_0/B , whereas the braids σ_i^{2k+1} have $(2k + 1)$ -times larger range of the cyclotron orbit Φ_k/B . In the case of a complete filling of the lowest Landau level (LLL), $N = N_0$ (where $N_0 = \frac{eBS}{h}$ is the degeneracy of the LL, N is the number of electrons, S is the surface-field of a system) gives $\frac{S}{N} = \frac{h}{eB}$ and the braids σ_i with the range Φ_0/B perfectly fit to interparticle spacing (electrons repulse themselves and keep fixed inter-distances on a positive homogeneous jellium) and these σ_i realize neighbor interchanges – then IQHE state is organized, $\nu = \frac{N}{N_0} = 1$. If, however, the external field increases e.g., three times, then the degeneracy proportional to the field also increases three times which gives the filling factor $\nu = 1/3$. The braids σ_i in so strong field are too short and do not reach neighboring particles, but the larger braids σ_i^3 with the range $\Phi_1/(3B)$ perfectly fit now to the electron spacing defined by $\frac{S}{N}$. Thus σ_i^3 are now the new generators of exchanges and they generate a subgroup of the full braid group, which we call as the cyclotron braid subgroup.

Wave functions of multi-particle interacting systems must transform according to a one-dimensional unitary representation (1DUR) of a braid when arguments of this functions interchanges according to this particular braid (these arguments correspond to classical positions of particles). For electrons (fermions) 1DUR $\sigma_i \rightarrow e^{i\pi}$, whereas for an exemplary cyclotron subgroup 1DUR $\sigma_i^3 \rightarrow e^{i3\pi}$, which gives exactly the Laughlin correlations for FQHE state at $\nu = 1/3$. This simplest example demonstrates what is a true reason of FQHE formation. The observed 'magic' hierarchy of LL fillings for FQHE results from the fact that the number of braid loops must be integer (then σ_i^{2k+1} with even exponential is a braid-exchange, thus can be a generator of a cyclotron subgroup). A collective correlated state (FQHE) arises only if braid-exchanges are admissible and the quantum statistics can be defined, i.e., when the braids perfectly fit to electron spacing (taking into account the nearest and next-nearest neighbors and multiloop braids), which leads to step-wise changing patterns of the commensurability defining discrete homotopy phase and corresponding hierarchy

²A space \mathcal{A} is simply connected if its fundamental homotopy group $\pi_1(\mathcal{A}) = \varepsilon$ (neutral element), i.e., is the trivial group (all closed trajectories – loops – can be contracted to a point in a simply connected space); a space \mathcal{A} is multiply connected if $\pi_1(\mathcal{A}) \neq \varepsilon$ (there exist topologically inequivalent trajectories in such a space).

³ $B_N = \pi_1(\Omega)$, $\Omega = (M^N - \Delta)/S_N$, where π_1 is the the first homotopy group (fundamental group), Ω is the configuration space of N indistinguishable particles on a manifold M (in our case $M = R^2$), Δ is a subset of diagonal points in N -fold product M^N , removed in order to preserve particle number conservation, and the quotient structure by the permutation group S_N introduces the indistinguishability of identical particles.

of FQHE.

Braids groups define the domain for integration over trajectories upon the scheme of Feynman path integral and the introduction of the cyclotron braid subgroups appears to be crucial for quantization in multiply connected spaces with magnetic field. This specific quantization can be precisely mathematically incorporated within the formalism of path integrals for many particle systems.

The sketched above scheme of this quantization can be generalized onto the whole scope of the Hall physics in various materials and explains in an utter manner the hierarchy of FQHE in the LLL and at fractional fillings of higher LLs, in conventional 2DEG GaAs, graphene monolayer and bilayer and even in the fractional topological Chern insulators (where magnetic field is replaced by a Berry field), taking into account also Hall metal states and Hall paired states. The developed topological theory of homotopy for FQHE explains all details of the fractional hierarchy observed experimentally, defines a method for construction of related trial wave functions allowing next the activation energy assessment. The latter occurs to be consistent with the numerical exact diagonalization of interaction on small models and with experimentally measured activation energies for particular Hall phases. The provided theory is a new explanation of FQHE, explains also hierarchy states beyond the reach of previous conventional models but being currently observed in experiments in growing details. The topological theory is able to identify an essence and constraints of former phenomenological models of FQHE, like composite fermion (CF) model or multi-component state theory of Halperin⁴. The topological theory is located within the formalism of Feynman path integral originally developed onto the case of multiply connected configuration spaces of multiparticle interacting systems with homotopy modified by a magnetic field (or Berry field). A remarkable result is a theoretical recovery for the first time of the longitudinal resistivity function, $R_{xx}(\nu)$, in Hall configuration in the LLL of 2DEG GaAs in consistence with its experimentally observed shape. It has been achieved by a development of the Feynman integral onto nonstationary states via summation over all competing in energy homotopy phases distinctly for varying ν . The method occurs also useful for explanation of complicated correlations in twin Hall systems with precluded or admitted interlayer tunneling of electrons. The detailed description of the entire achievement is presented below.

2 Detailed description

2.1 Introduction

The scientific achievement entitled "*Topological quantum effects in multiply connected 2D spaces and applications to Hall physics in 2DEG GaAs and in graphene monolayer and bilayer*" embraces 14 publications w international journals [1–15]⁵ and one monograph (World Scientific) [16] (averaged IF of [1, 2, 5, 6, 9, 12, 13] equals to 3.3). Publications presented as the scientific achievement are selected from 29 publications of the author within this topic [1–29] (24 after PhD). The monograph [16] published in 2012 has developed and summarized in its part (ca. 50%) the status of the model considered earlier by the author in his PhD thesis (2011) [18, 23, 24, 26, 27] and is a start-point for further development of the theory. The publications included to the achievement [1–15] are definitely different in their scope, especially concerning graphene, higher LLs and bilayer Hall systems. The achievement concerns a novel development of homotopy group application in formalism of Feynman path integral in multiply connected configuration spaces of many interacting charged particles in 2D exposed to strong magnetic field. We demonstrate that at sufficiently strong magnetic field in

⁴The crucial fact of the change of the magnetic field flux quantum in multiply connected spaces has been overlooked in former local non-topological descriptions of FQHE, which had to make use of some artificial objects like CFs, instead.

⁵In this reference list [8] is added separately for a convenience in citations.

such systems takes place a specific, different than the conventional one, quantization of magnetic field flux resulting in quantum homotopy phase transitions. Different homotopy phases define different correlation patterns induced by Coulomb interaction accommodated to varying quantization conditions. Homotopy description of planar system behavior appears to be convenient for explanation of some unclear previously aspects of FQHE in GaAs 2DEG and especially in graphene monolayer and bilayer. In the latter case, the observed recently (2016 [30]) unconventional FQHE can be just explained by topological model [2], supporting in this way a belief in the central role of the homotopy in organization of correlated states of 2D electron liquid exposed to a quantizing magnetic field.

The experimental discovery of FQHE by Tsui, Störmer and Gossard in 1982 [31] and defining of an appropriate multiparticle wave function by Laughlin 1983 [32] were recognized as the one of the most important accomplishments in condensed matter physics (Nobel prize 1998, Tsui, Störmer, Laughlin), because after half century since formulation of quantum mechanics it has been encountered a quantum phenomenon exceeding its accepted framework, which is apparently linked with an unconventional nonlocal topological character of FQHE. This phenomenon manifests itself by puzzling fractional hierarchy of LL fillings for FQHE, $\nu = \frac{N}{N_0}$ (N number of electrons, N_0 degeneracy of LL) with similar as for IQHE Hall resistivity quantization, $R_{xy} = h/e^2\nu$, and with vanishing longitudinal resistivity R_{xx} . This hierarchy is surprisingly universal despite quite different microscopic material realizations of Hall systems (e.g., in GaAs [33] or in graphene [30, 34, 35], or even in fractional topological Chern insulator without a homogeneous magnetic field [36–38]), when the common their property is just the similar homotopy of trajectories in appropriate Feynman integral. Despite many attempts the reason of specific correlations manifesting as FQHE has not been identified upon the local (non-topological) quantum mechanics. Instead, these correlations have been phenomenologically described in part in terms of composite fermions (CFs) [39]. CFs utilize a fictitious auxiliary field, flux quanta of it are assumed to be pinned to electrons and reproduce Laughlin phase correlations due to Aharonov-Bohm-type effect [40, 41]. Let us, however, note that the effectiveness of CF model evidences its implicate topological character. Despite declaration [40], CFs are not quasiparticles, they are rather nonlocal objects, since both flux quanta 'pinned' to electrons and Aharonov-Bohm phase shift are nonlocal notions closely related to trajectories. Pictorial model of CFs occurs usable especially due to a mapping of fractionally filled LLL states onto higher LLs completely filled in an resultant field diminished by an averaged field of auxiliary fluxes, which successfully reproduces a main part of FQHE hierarchy in the LLL [40]. However, there appeared recently many new observations both in GaAs 2DEG [33, 42–45] and mostly in graphene [30, 34, 35, 46, 47] going apparently beyond the explanation ability of the conventional CF model. Especially controversial in this respect occur Hall experiments in bilayer graphene [30, 35, 48].

Besides CFs also other models for FQHE phenomenon were formulated, like HH hierarchy (Haldane, Halperin [49, 50]), or multicomponent generalization of Laughlin function (Halperin [51]). The HH hierarchy (of succeeding generations of anyons) has been early abandoned because of its unrealistic property (too quickly growth of wave function size for succeeding anyon generations going beyond the size of the system) [49], whereas the multicomponent Halperin states quite well, though in a selective manner, coincide with exact diagonalization in small systems on Haldane sphere or torus [52–54], competing with the CF model, but also not elucidating an essence of FQHE phenomenon. In turn, the demonstration by Haldane [36] (included in part to his Nobel prize 2016) of the IQHE without Landau levels emphasizes a significance of formerly noticed topological conditioning of Hall physics [32, 55]. It has been noticed also a typical FQHE hierarchy in numerical simulations of topological Chern insulators without a magnetic field and LLs, but at the same fractional fillings of flattened band counted by filling of 2D crystal lattice nodes [37, 38], which strongly emphasizes an universal character of FQHE in various 2D systems.

The main goal of the presented achievement is the formulation of mathematically rigorous topological

model of 2D multi-electron systems with interaction and controlled by an external quantizing factor, which allows for clarifying FQHE hierarchy and its universal character in agreement with experimental observations in various materials listed above.

The topological formulation [1, 2, 5, 8, 16] solves the essential problem in Hall physics – the manifestation of the same hierarchy of FQHE despite significant differences between various systems (GaAs, graphene and other). The reason of this experimental fact is hidden and was not identified within local approaches, as e.g., in exact diagonalizations of interaction. The misleading conclusion frequently formulated was that the single particle LL states decide on hierarchy resulted from the exact diagonalization of interaction, because these states span the basis in the Hilbert space for the algebraic diagonalization. The reason of fractional hierarchy is another one, actually. We concluded that the decisive factor is a commensurability of cyclotron orbits with particle separation kept fixed by interaction – this is implicitly involved also in numerical diagonalization of the interaction – the number of electrons is rigidly fixed (at most 20 because of numerical efficiency limit [52–54, 56]) similarly as the system surface also rigidly fixed, whereas B field value and LL number define cyclotron orbit size. The hierarchy is selected independently of single-particle Landau state shapes. The latter decide only on the energy gap value (activation energy for states selected by the commensurability condition). This is better visible in Feynman path integral approach, because the commensurability enters the integral explicitly with summation over homotopy classes. The latter is apparently conditioned by Coulomb interaction of electrons as the commensurability concerns only interacting systems. The interaction enters also the path integral via another channel – via Lagrangian in exponential with the action. This channel is 'equivalent' to 'net' diagonalization of interaction but the first one is crucial for FQHE hierarchy. In the exact diagonalization⁶ both channels for interaction are also present, though the first one is hidden (enters the numerical calculus implicitly), which causes a misinterpretation in the literature regarding the actual conditioning of the fractional hierarchy [53, 54].

$$\langle z_1, \dots, z_N \left| e^{-i\hat{H}(t'-t)/\hbar} \right| z'_1, \dots, z'_N \rangle = \sum_{l \in \pi_1} e^{i\alpha_l} \int d\lambda_l e^{iS[\lambda_l]/\hbar}, \quad S[\lambda_l] = \int_t^{t'} L[\lambda_l] dt, \quad L = T + V$$

Fig. 1: Figuratively marked two channels for the entering of electron interaction in the Feynman path integral for Hall system (λ_l denotes a trajectory linking initial, z_1, \dots, z_N at t , and final, z'_1, \dots, z'_N at t' , points in the configuration space of N indistinguishable particles in l -th sector of the domain with local path measure $d\lambda_l$, π_1 is the braid group enumerating sectors in the path domain, $e^{i\alpha_l}$ is the one-dimensional unitary representation of the braid group, $S[\lambda_l]$ is the classical action functional, L is the classical Lagrangian, \hat{H} is the quantum Hamiltonian.

2.2 The rules of the proposed topological model

A start point for the topological model is the fundamental homotopy group $\pi_1(\mathcal{A})$ [16, 57, 58], which is a collection of disjoint loop classes in the space \mathcal{A} , which cannot be transformed one into another one by a continuous deformation. For \mathcal{A} being the configuration space of N indistinguishable particles on a plane, π_1 is an infinite countable group called as the full braid group B_N (Artin group) [57], quite different than π_1 for the configuration of N indistinguishable particles in 3D space (or in higher dimensions), where π_1 is finite permutation group S_N . This exceptional rich structure of trajectory homotopies in 2D (on plane, and

⁶Exact diagonalization in Hall systems [53, 54] consists in diagonalization of the matrix of interaction in the basis of anti-symmetrized products of single-particle Landau states taken from selected LL; this is a standardized numerical procedure, cf. e.g., the library of codes <http://www.nick-ux.org/diagram/index.php?LG=en>.

also on locally 2D manifolds, like sphere or torus [16,59]) stands behind the exotic Hall physics in 2D.

Trajectories of many particles on a plane entangle together creating braids (hence the name of group) in a manner non-encountered in higher dimensions and it concerns also closed loops in the configuration space of indistinguishable particles building π_1 [16, 57, 60]. Loops correspond here with exchanges – the transformations of the whole system when initial and final points differ only via reenumeration of particle indices. More formally [16, 57, 58]), $B_N = \pi_1(\Omega)$, where $\Omega = (M^N - \Delta)/S_N$ is the configuration space of N indistinguishable particles on a manifold M (here $M = R^2$), Δ is the set of diagonal points in the product M^N , subtracted to ensure particle number conservation, the division by S_N (permutation group) ensures indistinguishability of particles [16,61]. Multiparticle wave function of the whole system, $\Psi(z_1, \dots, z_N)$, must transform according to one-dimensional unitary representation (1DUR) of B_N element if arguments of this function mutually exchanges according to this element – a particular braid [60,62–64]. In the wave function $\Psi(z_1, \dots, z_N)$, $z_i = x_i + iy_i$ is the position of i -th particle represented on the complex plane. These arguments are classical positions of particles. While in 3D exchanges of particles correspond only to permutations of indices, in 2D exchanges depend also of trajectories expressed by braids. Always important are 1DURs of particular braids, which determine quantum statistics. Various statistics are as many as different 1DURs exist [63, 64]. In 3D the permutation group being the braid group in 3D has only two different 1DURs corresponding to bosons and fermions. In 2D there exist infinite number of 1DURs defining anyons [55,63]. It was known previously [55,60,62,63] but not exhausted a plethora of homotopy of 2D interacting electrons especially in the presence of a strong quantizing magnetic field, as presented in the achievement.

2.3 Cyclotron braid subgroups

An essential result of the author is a discovery that in the case of quantizing magnetic fields perpendicular to the plane with interacting electrons, the full braid group must be substituted by its subgroup, if cyclotron orbits are shorter than the interparticle separation kept fixed by Coulomb electron repulsion (classical electrons create a triangle Wigner net at $T = 0$ K, it is an energy lowest classical state of electrons on a positive 2D jellium). At magnetic field presence braids must be built from half-pieces of cyclotron orbits – non other trajectory exist [7,16,18,23,27]. In 2D cyclotron orbits are of finite size (in contrary to 3D where cyclotron orbits can be arbitrary long due to a helical movement). Thus 2D braids are also confined in size and cannot match neighboring particles if field is too strong [1,16]. When braids cannot be defined (implemented) then the statistics cannot be determined – it is blocked by the homotopy constraint. Too short braids must be removed from the braid group. In 2D it occurs, however, an exceptional opportunity – multiloop trajectories have a larger size. This fact has been proved by the author [1,7]. Multiloop braids are present in the full braid group because of its algebraic structure. The full braid group is generated by the generators σ_i , i.e., elementary exchanges of neighboring particles i -th with $(i + 1)$ -th ones without any additional loops. The full braid group elements, σ_i^{2k+1} , are also exchanges but with additional k loops [8,16,27]. These braids are larger, they take a role of elementary exchanges at strong enough magnetic field, and generate a subgroup of the former full braid group. This subgroup we call as the cyclotron braid subgroup [7,8,16]. Its elements are multiloop braids, which:

1. match electrons too distant for ordinary loop-less braids,
2. have 1DURs exactly as needed to explain exotic Laughlin correlations.

The property 1. follows from the geometry 2D, when the flux of external magnetic field must be divided/distributed among all loops of the multiloop cyclotron orbit (half-piece of cyclotron orbit defines a braid, thus for k loops in the braid we deal with $2k + 1$ loops in the corresponding cyclotron orbit). In 2D all loops share a common surface which results in division of an external flux into pieces, quite opposite to

3D where each loop has its own surface and adds to the total flux. This causes an increase of the multi-loop orbit size in 2D [1, 8, 16]. This fact has been proved by the author via formal generalization of the Bohr-Sommerfeld rule onto the case of multiply connected space [1]. According to this proof it has been shown that x, y components of the kinematic momentum at z oriented magnetic field are canonically conjugated variables for which Bohr-Sommerfeld rule defines the magnetic field flux quantum. In multiply-connected space this flux quantum is $(2k + 1)\frac{h}{e}$, where k is the number of loops in the braid (or $2k + 1$ is the number of loops in cyclotron orbit [8, 16, 27]). The orbit size is equal to $(2k + 1)\frac{h}{eB}$ – is greater than $\frac{h}{eB}$.

The property 2. follows from the form of the 1DUR for a cyclotron subgroup [9, 16, 23]: $\sigma_l^{2k+1} \rightarrow e^{i(2k+1)\pi}$ when we have chosen $\sigma_l \rightarrow e^{i\pi}$, t.j. $\alpha = \pi$ as for ordinary fermions from the general 1DUR, $e^{i\alpha}$ (i.e., $\alpha = \pi$). In this way we get Laughlin phase shift $(2k + 1)\pi$ acquired by the Laughlin function when particles interchange. We have thus shown that CFs represent only pictorially, by means of fictitious field flux quanta attached to electrons, additional cyclotron (braid) loops – one additional loop per one flux quantum attached. The Laughlin phase is naturally given by 1DUR of the cyclotron subgroup without any need to invoke to Aharonov-Bohm effect⁷.

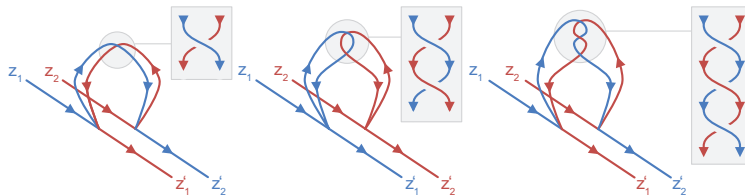


Fig. 2: Examples for attachment of various braids to multiparticle trajectories – braids are nonhomotopic, thus the domain of the path integral decomposes into disjoint homotopy-inequivalent sectors

2.4 Location of cyclotron braid subgroups within formalism of Feynman path integral

The presented cyclotron braid theory has a rigorous formal character in mathematical homotopy terms of π_1 group [58]. This approach invokes to Feynman path integrals [65, 66] if applied to quantum description of multi-particle system with interaction. Feynman integral defines the propagator, i.e., the complex matrix element of the evolution operator in the position representation (Fig. 1). The path integral over all classical trajectories must be supplemented (in the case of a multiply connected configuration space [58], for $\pi_1 \neq \varepsilon$) with additional summation over the braid group, because to each open trajectory in path integral can be attached a braid loop in any point (Fig. 2) which causes the decomposition of the full path domain into nonhomotopic sectors. Because of the discontinuity between sectors it is impossible to define the path measure over the whole domain but it can be done only separately on disjoint sectors [1, 7, 8]. Path integral acquires thus the additional summation over braid group with unitary (owing to causality) weights. It has been shown that these weights form 1DURs of the braid group [64]. In the case of 2D electrons upon the strong magnetic field the proper braid group is the cyclotron braid subgroup [1, 6, 14, 16, 26]. The 1DURs defines quantum statistics [55, 60, 64], including those for fractional LL fillings corresponding to FQHE. The latter states are possible only when multiloop orbits (braids) reach neighboring particles (including nearest and next-nearest neighbors) – this happens exclusively at discrete ‘magic’ fractional values of LL fillings

⁷It is clear that auxiliary flux quanta cannot be literally pinned to electrons because fluxes are quasiclassical or classical objects unavoidably related with trajectories – for flux quanta still with finite trajectory size, either with infinite non-realistic field. Thus the treatment of CFs as quasiparticles [40] is only pictorial.

$\nu = \frac{N}{N_0}$ (N number of particles, $N_0 = \frac{BS_e}{h}$ degeneracy of LL), because of commensurability restrictions⁸. Due to these restrictions it arises a specific fractional structure of fillings – the hierarchy of FQHE (observed in ca. 150 details in conventional 2DEG GaAs and in graphene). The prerequisite for the commensurability is the interaction and related correlations can be organized only in interacting multi-particle systems. The structure of this commensurability (detailed in series of author papers [2,5–9,11–16,27]) is perfectly consistent with experimentally observed FQHE hierarchy including also those out of reach of conventional CF model but visible in experiments. The commensurability may concern nearest or next-nearest neighbors. We have proved that commensurabilities with next-nearest neighbors (for multiloop as well as for single-loop cyclotron orbits) cannot be accounted for in a conventional CF model.

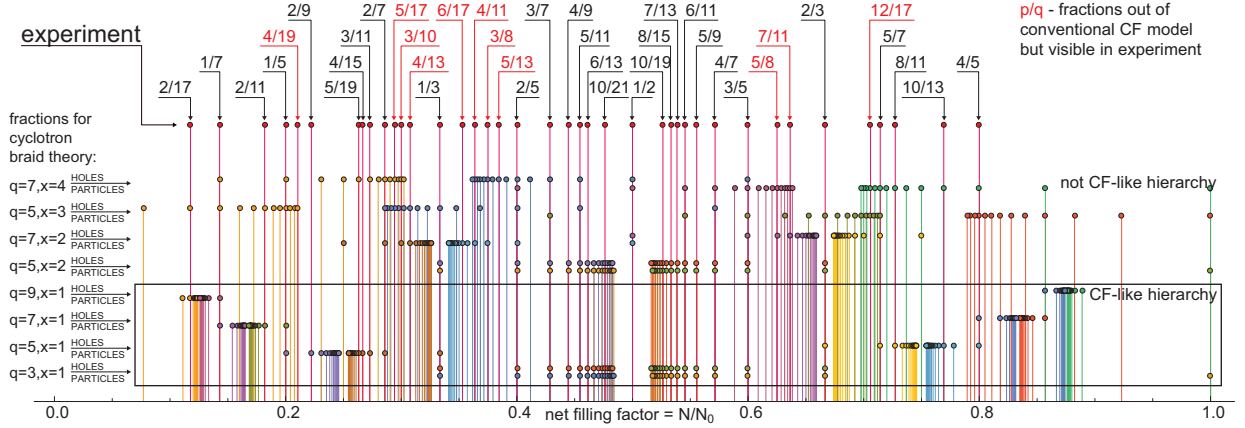


Fig. 3: Comparison of experimentally observed FQHE hierarchy in LLL (GaAs) with the general braid group hierarchy $\nu = \frac{xy}{(q-1)y \pm x}$, CF hierarchy $\nu = \frac{y}{(q-1)y \pm 1}$, indicated by red frame (bottom), rations marked with red color correspond to so-called *enigmatic* states not present in CF hierarchy (Hall metal in w 1/2 is marked) [1, 8]

The discrete fractional hierarchy resulted from the braid commensurability resembles to some extent also fractal dispersion of Landau levels in 2D crystal (considered in 60. by Azbel [67] and illustrated next graphically as the Hofstadter butterfly [68]), which displayed the commensurability of cyclotron Landau orbits with elementary crystal cell size. In the case of FQHE the commensurability of cyclotron Landau orbits refers to the Wigner crystal of electrons themselves. The scale of this lattice is given by the magnetic length $l_B = \sqrt{\frac{\hbar}{eB}}$. For B corresponding to $\nu = 1$ in GaAs, $l_B \simeq 10$ nm, and is ca. two orders larger than the scale of ordinary crystal, hence the cyclotron commensurability in Wigner crystal manifests itself via FQHE at field of order of 20 T, whereas observation of the Hofstadter butterfly required unrealistic field $\sim 10^5$ T, at lattice constant ~ 0.2 nm. Moreover it should be emphasized that the hierarchy of Hofstadter-Azbel had not a physical foundations related to the commensurability which was there rather abstract. In the case of FQHE this insufficiency is filled with the multiloop homotopy trajectory structure defining simultaneously quantum statistics via 1DURs of cyclotron braid subgroups. Moreover, the fractal structure of Landau sublevels in the case of Hofstadter butterfly is a single-particle effect⁹, whereas cyclotron braid commensurability is an collective phenomenon with the essential role of interaction (the Wigner crystal of electrons arises only due to electron repulsion). Multiloop braid is also a notion beyond Hofstadter-Azbel illustration. Thus

⁸The degeneracy of LLs is here an important factor because perfectly flattened band guaranties homogeneity of cyclotron orbits conditioning the commensurability. This condition is fulfilled in 2DEG GaAs and in graphene monolayer or bilayer, because the LL degeneracy is originated by ladder operators of oscillator [16] independently of different crystal field in various materials (for a Chern insulator with flattened band the degeneracy is equal to number of elementary cells).

⁹For commensurability of Hofstadter-Azbel [67, 68] it has been considered an abstract comparison of cyclotron orbit and elementary cell sizes – both characteristics are single-particle without any influence of the interaction.

the relation of it with homotopy cyclotron theory is rather indirect only via emphasizing the general role of the commensurability (e.g., the considered fractal structure of the Hofstadter butterfly for irrational commensurability ratio [68] has any counterpart in always countable cyclotron braid commensurability).

2.5 Symmetry of multiparticle quantum states according to cyclotron braid model, trial wave functions and their energy

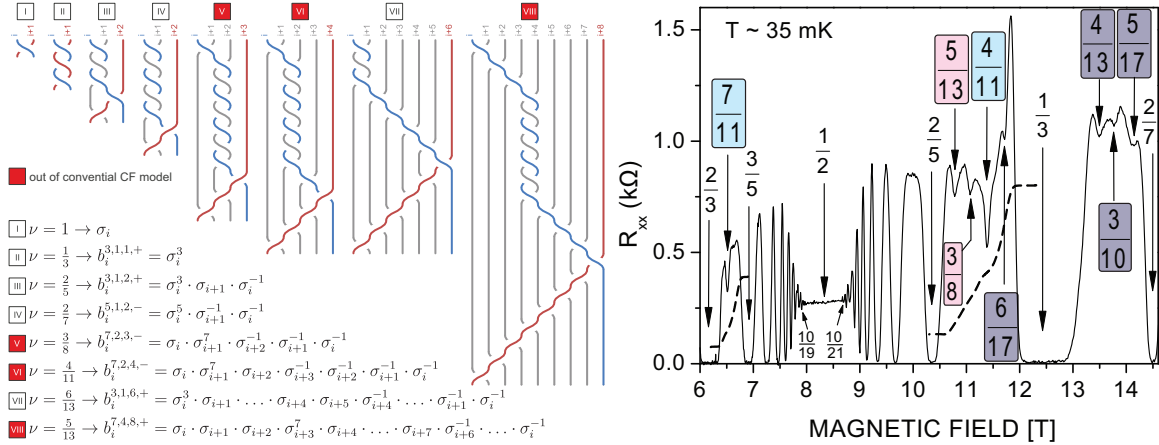


Fig. 4: Few examples of cyclotron braid generators [8] (including *enigmatic* states, the latter are fixed with color on the experimental longitudinal resistivity R_{xx} [33]); similar depth of local minima on the $R_{xx}(\nu)$ curve was also explained by the braid model [1, 8]

Unitary representation (1DUR) of a cyclotron braid subgroup is governed by the commensurability pattern defining generators of this subgroup. When a specific filling factor, $\nu = \frac{N}{N_0}$, ($N_0 = \frac{BS_e}{h}$, S and N are kept constant and only field B variates) admits some commensurability scheme (i.e., this factor ν belongs to the FQHE hierarchy), then one can identify the form of generators (elementary exchanges of particles), which next defines 1DUR on these generators (taking into account that for original electrons 1DUR $\sigma_i \rightarrow e^{i\pi}$). The deciding factor is the number of loops in a particular cyclotron braid subgroup generator, which typically gives 1DUR $e^{i(2k+1)\pi}$ or $e^{i(2k-1)\pi}$ (the latter for the commensurability pattern with the last loop inverted, i.e., of eight-figure form). The specific form of the commensurability defines, however, also properties of all loops in a multiloop structure and reflexes the range of each loop including next-nearest neighbors ($y \geq x \geq 1$ in the general braid group hierarchy in the LLL, $\nu = \frac{yx}{(q-1)y \pm x}$, $q = 2k + 1$). This corresponds to decomposition of all electrons into subsets of next-nearest neighbors of order of x and y (taking into account that each particle has neighbors of an arbitrary order, in thermodynamic limit) and induces the related form of a generalized multicomponent Laughlin function. We note that exchanges are confined to these subsets preserving cyclotron 1DUR symmetry, whereas intergroup exchanges are not admitted. This causes an interesting property of partial infringement of the function antisymmetry on specific subsets of next-nearest neighbors. We must remember that a cyclotron group and its unitary representation define the specific quantum statistics, and we have found that for original fermions, cyclotron braids repeat antisymmetry though not for all electron exchanges but only for those in the subsets defined by a specific commensurability pattern¹⁰. Generators and their 1DURs allow thus for the modeling of corresponding multiparticle wave functions. In the LLL the symmetry properties allow for unique definition of the polynomial part of a wave function obligatory holomorphic in $n = 0$ LL [52]. The method agrees on the family of Laughlin functions and allows for further generalization. Trial wave functions constructed for filling factors corresponding to

¹⁰For many ν none commensurability is admitted, whereas FQHE occurs only at discrete 'magic' hierarchy of fillings.

commensurability patterns allow next for assessment of the related energy of correlated states by utilization of Metropolis Monte Carlo method [69, 70]. The calculated energies [1, 2, 13, 15] for various filling rates and for relatively large number of electrons (up to 600) very well agree with exact diagonalization of interaction in small models and with experimentally measured activation energy (some examples are shown in Table 1).

q	x	y	hierarchy fraction, $\nu = \frac{yx}{(q-1)y \pm x}$	energy from Monte Carlo simulation for functions given by braid model	energy from exact diagonalization
3	1	2	$\frac{2 \cdot 1}{(3-1) \cdot 2 + 1} = \frac{2}{5}$	-0.432677	-0,432804
3	1	3	$\frac{3 \cdot 1}{(3-1) \cdot 3 + 1} = \frac{3}{7}$	-0.441974	-0,442281
3	1	4	$\frac{4 \cdot 1}{(3-1) \cdot 4 + 1} = \frac{4}{9}$	-0.446474	-0,447442
3	1	5	$\frac{5 \cdot 1}{(3-1) \cdot 5 + 1} = \frac{5}{11}$	-0.451056	-0,450797
5	1	2	$\frac{2 \cdot 1}{(5-1) \cdot 2 + 1} = \frac{2}{9}$	-0.342379	-0,342742
5	1	3	$\frac{3 \cdot 1}{(5-1) \cdot 3 + 1} = \frac{3}{13}$	-0.348134	-0,348349
5	1	4	$\frac{4 \cdot 1}{(5-1) \cdot 4 + 1} = \frac{4}{17}$	-0.351857	-0,351189

Table 1: Comparison of energy values obtained by exact diagonalization and by Monte Carlo simulation for some exemplary filling fractions for FQHE (Monte Carlo Metropolis simulation for proposed topology based wave functions, for 200 particles) [1, 8]

2.6 Explanation of *enigmatic* hierarchy of FQHE in the LLL out of conventional CF hierarchy; limits of CF model applicability

The developed topological braid group approach to FQHE seems to be universal and can be applied to various materials, in the LLL and in higher LLs (in higher LLs experimental observations reveal the FQHE which do not repeat a pattern from the LLL [42] because in higher LLs commensurate orbits are typically single-loop [11] not present in the LLL, out of reach for CF model, but still handled in braid terms).

The author proved that so-called Jain hierarchy of CFs in the LLL, $\nu = \frac{y}{(q-1)y \pm 1}$, where $y = 1, 2, \dots$ and q – an odd integer [40], corresponds to the braid model commensurability of multiloop orbits only for nearest neighbors, i.e., it corresponds to the general braid hierarchy [1, 8, 15], $\nu = \frac{yx}{(q-1)y \pm x}$, taken for $x = 1$ (which means the commensurability correlation of only nearest neighbors for $q - 1$ first loops of q -loop cyclotron orbit). However, the large number of FQHE fillings experimentally observed [33, 71] is placed out the Jain hierarchy, e.g., $\nu = \frac{3}{8}, \frac{3}{10}, \frac{4}{11}, \frac{5}{13}, \frac{7}{11}, \frac{6}{17}, \frac{4}{13}, \frac{5}{17}, \dots$. These fractions are called in the literature as *enigmatic hierarchy* and this hierarchy in a direct way results from commensurability braid conditions with next-nearest neighbors ($x > 1$), not accounted for by CFs. Though, there are proposed generalizations of CF model toward 'interacting CFs', when the next generation of CFs is constructed due to once more attachment of flux quanta to already dressed with flux quanta lower generation CFs, but such an approach needs new phenomenological assumptions. Arising of the needed here strong 'residual interaction of CFs' in a step-wise way due to a tiny change of the filling factor seems to be not justified physically, and is rather a next speculative auxiliary/artificial assumption (this residual interaction is not microscopically explained and it exceeds even the original Coulomb interaction strength) [72]. This approach encounters problems with justification why these next generation CF interaction would occur suddenly for CFs already dressed with Coulomb interaction [39, 40] and originally considered as quasiparticles¹¹.

¹¹Quasiparticles are defined as poles of the single-particle retarded Green function (as in a model case of Landau quasiparticles in metal [73]), which needs continuity of the mass operator near the Fermi surface [73] – this requirement in 2D Hall systems seems to be problematic because of the discontinuity of the mass operator induced by the interaction (discontinuity with respect

Nevertheless, the predictions of the topological braid model agree in a natural way with observations also of enigmatic hierarchy [1, 8, 15], and the step-wise changes of the commensurability is a natural related property needfully discrete one (it follows thus, that CFs may be treated as an effective model of multiloop braids but only for commensurability of nearest neighbors, i.e., when $x = 1$ in the above formula). Good agreement of energy of trial wave functions in CF model with exact diagonalization is linked with its equivalence to the braid model at $x = 1$ and with a semi-empirical variational method to optimize energy via choice of the scheme of projection from higher LLs onto the LLL, essential in Jain method [40] and necessary to obtain a required holomorphic function in the LLL from a nonholomorphic one in higher LLs. This projection is not uniquely defined and usually does not conserve symmetry in contrary to mathematically rigorous form of generators of cyclotron braid subgroups defining this symmetry¹². The variational energy may closely approach the exact one, but an uncontrolled procedure of the projection onto LLL perturbs symmetry and correlations, which can be visualized by drawing Pauli crystal portraits for correlations defined by various trial wave functions [13]. The virtual Pauli crystal displays a 'detailed distribution' of particles according a given trial wave function. The numerical method (of Metropolis Monte-Carlo-type) determines the most probable position configuration in 2, 3, 4, 5, ... electron clusters in a strongly correlated multi-particle system [13, 15] and pictorially reveals differences between topological approach and CF projections onto LLL perturbing the exact symmetry required by 1DURs of cyclotron braid generators. It may be added that the correlation visualization by a virtual Pauli crystal corresponds to a detailed equilibrium in thermodynamics, where various particular distributions are equivalent, though are characteristic to a type of correlation under consideration. The Pauli crystal is only virtual one and does not display any local crystal ordering but may be helpful in visualization of correlations¹³, which was illustrated in the author paper [13].

2.7 Structure of single-loop FQHE states in higher LLs

In higher LLs a more complicated braid commensurability patterns exist in comparison to the LLL and this fact meets with experiments and allows for explanation of FQHE hierarchy quite different in higher LLs than in the LLL, observed in GaAs [42] and in w graphene [30, 34]. The reason of this oddness is that single-loop cyclotron orbits are always shorter than particle separation only in the LLL, but in higher LLs cyclotron orbits are larger for lower magnetic field and for larger kinetical energy, $(2n + 1)\frac{\hbar\omega_B}{2}$, for $n > 0$. The cyclotron orbits and braids built from their half-pieces are in higher LLs usually longer than particle separation quite opposite to the LLL (with exception to fillings close to LL band edges, with small occupation there and larger dilution of particles). The topological braid model solves this problem – now of too long cyclotron orbits – by commensurability of single-loop long orbits with next-nearest neighbors, which leads to a hierarchy fully consistent with experimental observations in higher LLs. The CF model is here unusable, because this model utilized flux quanta pinned to electrons which mimics multiloop orbits with larger size – this is not needed in higher LLs, where even single-loop orbits are typically too long. In higher LLs the single-loop orbits matching next neighbors define FQHE and this new class of FQHE correlations proposed originally by the author [11] has been identified in higher LLs both in 2DEG GaAS and in graphene [2, 5, 8] in complete consistence with experiment (it is an important and new component of the presented scientific

to angular momentum, named by Laughlin as the electron spacing quantization [32].

¹²Higher LLs in construction of CF wave functions indicate implicitly correlations with next neighbors, typical for higher LLs, but in CF method only by last loop (to which is referred y in the above formulae) whereas the former $q - 1$ loops are blocked on the nearest neighbors by the condition $x = 1$, which strongly confines the CF model.

¹³It is defined according to a trial multiparticle wave function via searching of the most probable position (a center of local maximum) of n -th particle upon the former positioning in a similar way of $n - 1$ particle in a cluster (starting from an arbitrary position of the first one).

achievement – for the first time derivation of the FQHE hierarchy in higher LLs).

By application of the braid commensurability in higher LLs we identify a hierarchy of single-loop FQHE states [11] not existing in the LLL. This is because of larger size of cyclotron orbits for $n > 0$ in comparison to $n = 0$. Nevertheless, in higher LLs close to the band edges, where the diluted carries (electrons in this LL band or symmetrically, Landau holes) can be distributed even more distantly than the large cyclotron orbits. In these sectors of Landau bands multiloop orbit again will be convenient to match neighbors, which means that the multiloop FQHE in higher LLs is pushed toward band edges the stronger the higher LL index n is [6, 7]. These families of states thronging in close vicinity of integer filling ratios are overshadowed by IQHE-reentrant [7].

Introduced by the author [11] the new concept of single-loop FQHE states for LL index $n > 0$ successfully explains experimental observation of series of states with denominator 3 (occurring as doublets $\nu = \alpha + \frac{1}{3}, \alpha + \frac{2}{3}$, $\alpha = 3, 4$) for LL subbands with $n = 1$ and series with denominators 5 (four symmetrically located, $\nu = \alpha + \frac{1}{5}, \alpha + \frac{2}{5}, \alpha + \frac{3}{5}, \alpha + \frac{4}{5}$, $\alpha = 5, 6$) in subbands with $n = 2$ in 2DEG GaAs (enumeration α distinguishes spin subbands) [42]. The new FQHE correlated states defined by the commensurability of single-loop orbits with next-nearest electrons are similar to those at IQHE but here at fractional fillings in higher LLs¹⁴ and with fractional quantization of Hall resistivity, $R_{xy} = \frac{h}{e^2\nu}$ similarly as for multiloop FQHE states. The identified single-loop complexes of states are distinctly visible in the experiment, Fig. 5 (they are not connected with CFs). Moreover, in the center of the single-loop FQHE complexes there are located states at fillings $\nu = \frac{5}{2}, \frac{7}{2}, \frac{9}{2}, \frac{11}{2}, \dots$ (Fig. 5), which according to the braid model are correlated states of electron pairs (in agreement with observations and numerical simulations for Pfaffian [56]), but not at $\nu = \frac{1}{2}, \frac{3}{2}$ (in two spin subbands of the LLL), at which the braid model predicts the Hall metal [6, 7] also in consistence with experiment¹⁵.

With growing Landau index n the structure of single-loop complexes of fillings also expands as $2n$ symmetrically located FQHE states at fractions with denominators $2n + 1$ around centrally-in-band placed paired state¹⁶. Such a structure perfectly repeated in succeeding subbands for $n > 0$ is indeed observed experimentally up to $n = 2$ [42] – Fig. 5. For higher n the braid model predicts smaller and smaller activation energy of correlated states because of lowering number of electrons participating in these correlations in consecutive subbands (the rest of electrons completely fills the lower subbands) – these lowering correlation energy is more and more easily overcome by the thermal chaos (even in mK scale FQHE states for $n > 2$ are not visible [42, 56]). One can add, that multiloop FQHE states for $n > 0$ pushed to vicinity of subband edges [7] are also invisible as obscured by the wide IQHE-reentrant¹⁷, what is noticeable in Fig. 5.

The cyclotron braid group model allows for identification of a complete hierarchy of Hall metal by taking the limit to infinity of the last loop size in any family of FQHE hierarchy (e.g., the limit $y \rightarrow \infty$ in above written out braid hierarchy in the LLL). The Hall metal occurs thus (in accordance with this limit in two

¹⁴These states are as stable as IQHE states [34], which supports the single-loop its character similar as of IQHE states.

¹⁵Paired states correspond to the situation when too short spacing between particles are enhancing by particle pairing (reducing their number twice). Cyclotron orbits for pair are of the same size as for single particle, because $\hbar\omega_B = \frac{\hbar eB}{m} = \frac{\hbar 2eB}{2m}$. For twice lower concentration of pairs the commensurability gives fractions $\nu = \frac{5}{2}, \frac{7}{2}, \frac{9}{2}, \frac{11}{2}, \dots$. It is clear that pairing is allowed only for $n > 0$ when cyclotron orbits are larger than particle separation. Hence, for fractions $\nu = \frac{1}{2}, \frac{3}{2}$ occur not paired states but the Hall metal, the later corresponding to the limit $v \rightarrow \infty$ in the general braid hierarchy.

¹⁶In the simplest case of Landau spin subbands the state of pairs should be triplet polarized along the field (resembling d phase of superfluid He³), which agrees with numerical simulation by Morf [56].

¹⁷The states IQHE-reentrant are characterized by the same R_{xy} quantization and vanishing of R_{xx} as for an integer ν but for different nominal filling rate in a continuous region around the nearest integer ν , symmetrically in both sides with respect to it (ranging even 20% deviation in nominal filling – Fig. 5). This phenomenon is caused by striping of a sample (or bubble creation) up to integer filing of stripes in which correlation energy prevails over electrostatic energy cost due to striping of electron distribution on the substrate uniform jellium.

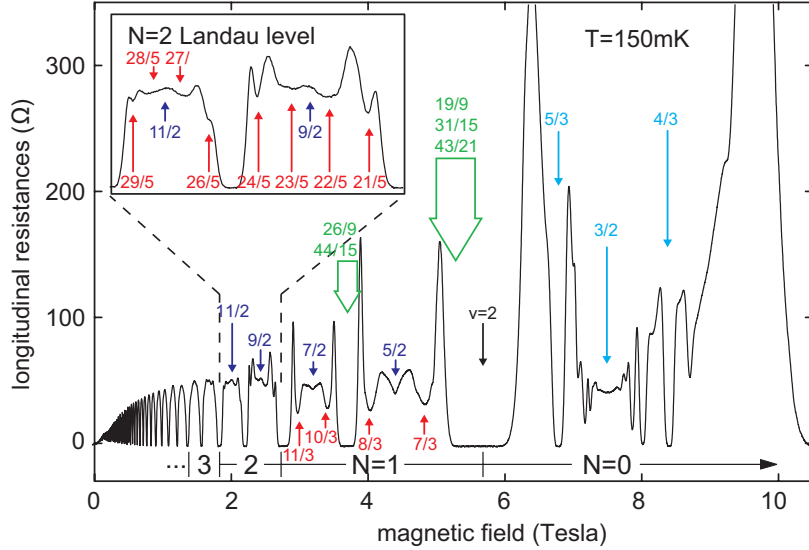


Fig. 5: Visible in experiment [42] single-loop FQHE state for Landau index $n = 1$ i $n = 2$ (N in fig.) (in GaAs) – indicated in red color; blue ones – $4/3$, $5/3$ are three-loop FQHE in LLL at $n = 0$; $\nu = 5/2, 7/2, 9/2, 11/2$ are paired states, but at $3/2$ is the Hall metal; by the green color are marked a few FQHE from multiloop series pushed toward band edges at $n > 0$ and obscured by IQHE-*reentrant* in vicinity of integer fillings [7, 11]

first LL spin subbands in the center of this subbands ($1/2$ and $3/2$), whereas it avoids central position in higher LL subbands (for $n > 0$, because in these subbands central their parts are occupied by single-loop FQHE states and connected with them paired states at half filling, in the subbands with $n > 0$ the Hall metal is pushed toward subband edges together with multiloop FQHE hierarchy the stronger-pushed the higher index n is). In the LLL the complete hierarchy of Hall metal is given by $\nu_{Hm} = \lim_{y \rightarrow \infty} \frac{xy}{(q-1)y \pm x} = \frac{x}{q-1}$. This hierarchy generalizes the CF hierarchy of Hall metal in the LLL, $\lim_{y \rightarrow \infty} \frac{y}{(q-1)y \pm 1} = \frac{1}{q-1}$, because CFs do not account all hierarchy families with $x > 1$ (of next-nearest neighbor contribution). It is noticeable that according to the braid model, Hall metal can occur (unexpectedly for CFs) also at odd denominator fractions (e.g., for $x > 1$ being an even number, e.g., 2, and then being the divider of $q - 1$ – always even number). Author described (for the first time) the complete hierarchy of Hall metal in GaAs and in graphene in the LLL and in higher LLs [2, 5, 8, 11] (in GaAs and in graphene).

In the next paper [10] it has been shown that the unavoidable condition for organization of FQHE correlations in any material is a sufficiently long mean free path of carriers, exceeding the size of a sample. Mobility proportional to the mean free path must be thus of order of 10^6 cm²/Vs for micrometer size of samples, which agrees with experiments. Especially important experimental demonstration [74] of the role of mean free path constraint is an experiment with annealing of the suspended graphene scraping (by short impulse of large current, removing impurities). The originally insulating sample after annealing became Hall correlated (FQHE at $1/3$). This astonishing experiment can be explained by the cyclotron braid model¹⁸. The sufficiently long mean free path is necessary for possibility of realization of long range braids in the cyclotron braid subgroup, which requires mobilities with mean free path exceeding the sample size [10, 16].

Note that braids and homotopy groups are purely classical notions and do not refer directly to quantum without-trajectory-dynamics. Topological classical archetype of the quantum system may or may not preclude some its real behavior, as e.g., in the case of 2D electrons in so strong field that classical cyclotron orbits are too short in comparison to electron separation. The similar situation concerns too small mean

¹⁸An annealing removes imperfections in the system and enhances mobility of electrons but does not change electron interaction – according CFs it should not change the stability of FQHE, in apparent contrast with the experiment [74].

free path precluding possibility of realization of large-distance braids. Both small or large braids are not quantum circumstances as are not quantum objects – braids are purely classical, but possibility or not of their organization precludes or admits corresponding quantum behavior. This illustrates an action of the topology in a quantum system. This action is not a direct one but reveals via conditioning premises only. Nevertheless, this indirect topological conditioning of quantum behavior via premises only is strong and deciding on experimental its manifestations (like Pauli principle for example). Illustrative is here the example with topological requirement of mean free path exceeding the sample size. Surprisingly, the larger range braids highly exceeding the system size (such braids also are present in any braid group) do not impose any additional constraint on the system, because such long braids never concern the finite quantum system and discussion of possibility of their realization is without any influence on real quantum system behavior (in opposition to braids lower than the system size). The similar character has also decision on applicability or not of perfectly 2D approach to actually 3D systems – again, it is important whether the real quantum system admit some topological premises or not. In this case such a premise is the large difference in energy of excitations for carriers in direction z in comparison to directions in-plane x, y , despite the 3D actual thickness of the quantum system. This illustrates the way of how the topology meets the quantum reality, the latter next accessible only via measurements. The channel of this implicit link topology-quantumness is the Feynman path integral. The presented achievement originally reveals this picture and illustrates it.

With the braid model there agrees also an observed stability of FQHE phase despite lowering electron interaction. This is visible in graphene (in fan diagrams) when reducing magnetic field and simultaneously the electron concentration in such a way that ν remains constant [2, 6, 34]. From the point of view of braid approach, at lower field cyclotron orbits are larger and fit to larger interparticle separation in more diluted electron liquid¹⁹. In CF model it is asserting a different role of the interaction, as a dress of electrons making them CFs, thus in CF terms, the stability of FQHE should diminish when the interaction weakened by dilution of electrons, which is, however, not observed [34]. We propose here an additional illustrating experiment, FQHE observation in dielectric surroundings (gaseous, liquid or solid) increasing an effective dielectric permittivity in Hall layer and reducing in this way electron-electron interaction. Observation of induced changes or not in FQHE stability (activation energy from Arrhenius plots of resistivity) might shed light on the true role of interaction (for graphene are accessible commensurate substrates with enormous high permittivity [75]). Another possible experiment might be [16] an experimental verification of cyclotron commensurability when passing $\nu = 1/2$, at which the cyclotron braid model forecasts reorientation for an inverse one (of eight-figure shape) of the last loop in the multiloop cyclotron orbit, upon development of previous experiments confirming cyclotron type of ballistic electron movement [16].

2.8 Application of the braid model to graphene monolayer

Utility of the braid model of FQHE and of cyclotron commensurability convincingly manifest themselves in interpretations of new experimental observations of FQHE [34] in higher LLs of monolayer graphene in subbands with $n = 1$ (up to sixth subband, taking into account spin-valley SU(4) degeneracy) and completely unclear and controversial observations of FQHE in bilayer graphene in eight consecutive subbands [30, 35, 48]. In the graphene case one must take into account and odd structure (pseudo-relativistic) of Landau levels resulting from specific band structure of graphene (an existence of Dirac cones in two inequivalent corners of hexagonal Brillouin zone). The SU(4) structure of spin-valley degeneracy in monolayer graphene and various schemes of its removal well model anomalous pseudo-relativistic IQHE [76] and allow for a development of

¹⁹In graphene one can change carrier concentration by a shift of the Fermi level in vicinity of Dirac points using a lateral voltage.

cyclotron braid theory of FQHE in this material.

Braid groups reflect topology of trajectories and not their dynamical particularities²⁰, hence, trajectory homotopy classes are governed in graphene by a bare kinetical energy the same as in conventional GaAs (with the same massive degeneracy in each subband despite the different crystal field)²¹. The braid FQHE hierarchy is modified in graphene by ordering of spin-valley subbands (four in each LL in monolayer graphene) and by a mirror-symmetry between valence and conduction bands with respect to the zero energy Dirac point. Simultaneously — what is most important — the same massive degeneracy is kept in each subband (the same as in GaAs). Agreement of braid group predictions with an experiment is convincing [34] — we have rederived one-to-one all observed in the experiment FQHE hierarchy details for $n = 1$ [2, 5, 6, 8, 9] — Fig. 6.

An interesting phenomenon is the absence in the experiment (as far as of yet) of enigmatic hierarchy series in the LLL of monolayer graphene, i.e, FQHE states at $\nu = \frac{3}{8}, \frac{3}{10}, \frac{4}{11}, \frac{5}{13}, \frac{5}{17}, \frac{6}{17}, \frac{7}{11}, \frac{4}{13}, \dots$ (perhaps the temperature should be more lowered to overcome the chaos). Astonishing is, however, an occurrence of similar series in the next four subbands (with $n = 1$) in monolayer graphene (visible at $T \simeq 50$ mK) [2, 6, 7, 34] (in graphene the details in higher LLs are better visible in experiment [30], which is not satisfactorily explained as of yet).

In monolayer graphene in subbands with $n = 1$ there are sharply visible doublets with denominator 3 [34, 78] — they are not CFs, but they are single-loop FQHE states (identified by us earlier for $n = 1$ in GaAs [11]) with commensurability of nearest and next-nearest neighbors in each doublet. Intensity of correlation manifestation diminishes with lowering number of electrons participating in correlations with growing number of subband, reducing the energy gain, which is visible in experiment with monolayer graphene (for $n = 1$ there are here 4 subbands and in the fourth one a signal is too small to be visible) [34] — this agrees with the braid model [2, 6]. The single-loop FQHE for $n = 1$ in graphene seems to be confirmed by strong its stability, similar as for also single-loop IQHE [2, 6, 34].

2.9 Explanation of an anomalous FQHE in bilayer graphene

The most important success of application of the cyclotron braid model is explanation of controversial observations of unconventional FQHE in bilayer graphene, completely different than in monolayer graphene [30, 35] (and not consistent with CF model). Recently there were observed ca. 30 FQHE features in the bilayer graphene in its subbands with $n = 2$ (with unprecedented accuracy and range up to eighth LL subband). The reason of the unconventional FQHE in bilayer graphene (even in its LLL) is the non-ideal two-dimensionality of the system — electrons can hop (tunnel) between two layers, which significantly modifies homotopy of trajectories and this can be precisely accounted for in cyclotron braid model with full agreement with experiment.

An inter-layer hopping of electrons in bilayer graphene causes the 'rounding' of Dirac cones (local bands in vicinity of Dirac points becomes in bilayer graphene again parabolic ones and the Landau spectrum attains the form $\sim \sqrt{n(n-1)}$ [77], whereas in monolayer graphene the local bands were pseudo-relativistic, locally linear in momentum, with the Landau spectrum $\sim \sqrt{n}$ [76], n — number of the oscillatory Landau state). From point of view of trajectory homotopy, the bilayer structure opens the possibility for escape of

²⁰If dynamics does not modify the homotopy — exceptionally, the perpendicular to basal plane magnetic field does not break cylindrical symmetry, thus, does not prefer and direction on the plane and may modify the homotopy by changing cyclotron orbit area, despite its detailed shape (not circular in interacting system). Nevertheless, other fields including electrical type crystal field, do not modify homotopy of trajectories.

²¹In conventional 2DEG GaAs, LL energy grows with n index as $\hbar\omega_B(n+1/2)$ (as in 2D gas), but in monolayer graphene as $\hbar\omega'\sqrt{n}$, $\omega' = 2v_F/l_B$ [76], and in bilayer graphene as $\hbar\omega_B\sqrt{n(n-1)}$ [77].

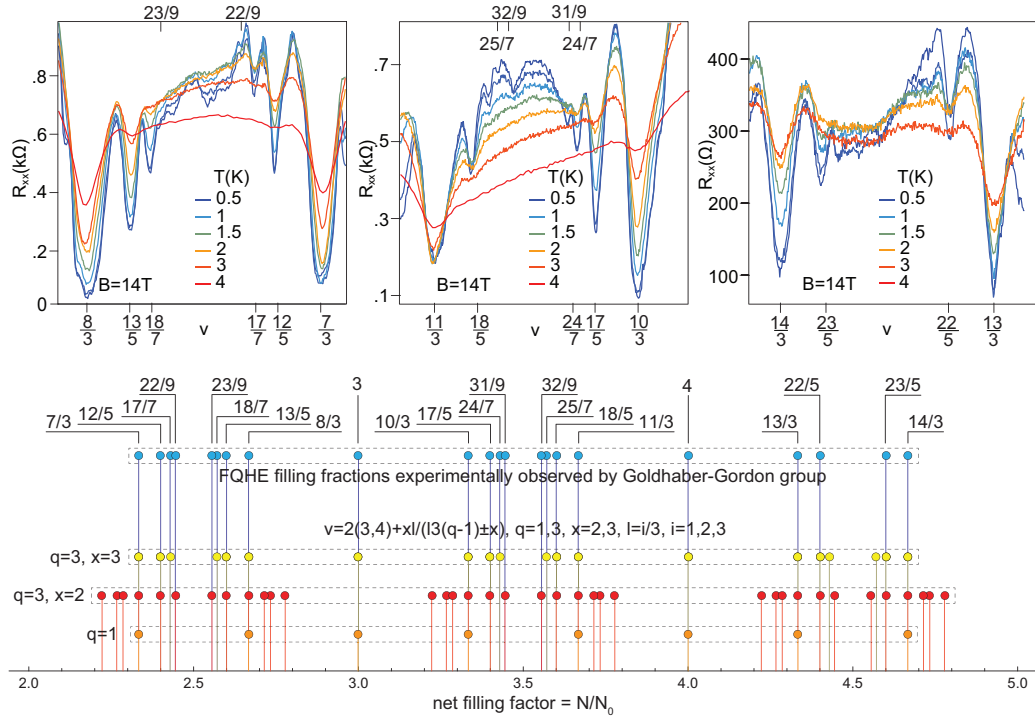


Fig. 6: Derived braid group hierarchy in monolayer graphene for $n = 1$ subbands [2, 6] with 1-1 agreement with the experimental observations (upper panels) [34]

one or more loops from one layer to opposite one (note that topology changes just due to new possibilities, not precluding others). If we deal e.g., with three-loop trajectory then the escape may realize $2 - 1$ or (equivalently) $1 - 2$ distribution of loops among layers – in both cases only 2 loops (and not all 3, as it was in monolayer) share the common flux of the external magnetic field, because the third loop in opposite layer has its own surface there. This causes that FQHE at $\nu = 1/3$, which was observed in monolayer Hall system, in the bilayer shifts to $\nu = 1/2$ (to the filling rate where in the monolayer was Hall metal) – and this phenomenon has been observed in the experiment [35]. This effect is not achievable in CF model (it needs loop manipulation among layers, and some proposed idea of division of attached flux quanta among layer is not consistent with the concept of CFs as quasiparticles [40]).

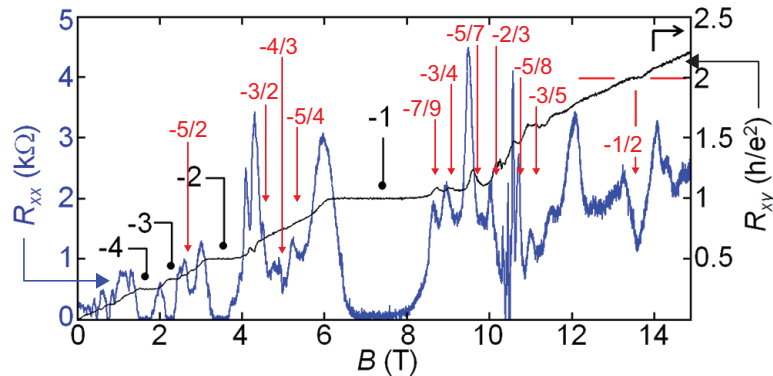


Fig. 7: FQHE features observed [35] in the LLL of bilayer-graphene in suspended sample, including most astonishing unusual FQHE filling at $\nu = -1/2$, caused by hopping of loop from multi-loop cyclotron trajectory to opposite layer (in red color the whole related to this hopping hierarchy is marked being in a very good consistence with the experiment [2])

Interesting that in a distinct experiment [48] (when bilayer graphene is supported by hexagonal hBN substrate instead of being suspended in air as in [35]) the FQHE state at $\nu = 1/2$ disappears – and here also the braid group model offers an explanation. In bilayer graphene one encounters an additional (called as 'accidental') degeneracy in the LLL of states with oscillatory Landau indices $n = 0$ and $n = 1$. These two states have in bilayer graphene the same energy, so both must belong to the LLL (it is a result of double annihilation operator in local Hamiltonian close to Dirac points, induced by interlayer hopping [77]). Together with spin-valley 4-fold degeneracy one arrives with 8-fold degeneracy of the LLL in bilayer graphene²².

But for $n = 1$ cyclotron orbits are 3 times larger than for $n = 0$ (at the same field B), and in the case when the subband with $n = 1$ is filled earlier than the subband $n = 0$, the three-loop orbit will be not needed and the hopping of a loop will not take place. The FQHE at $\nu = 1/2$ will here disappear, which explains the difference in observations in both experiments [2, 9, 14]. FQHE at $1/2$ occurs when the subband with $n = 0$ is filled first. The order of filling is inverted by a perturbation caused by the hBN substrate. Besides the state at $\nu = 1/2$, the braid model predicted a whole series of fillings in the LLL of bilayer graphene coinciding with experimental features – as shown in Fig. 8 (for $n = 0, 1$ order of filling).

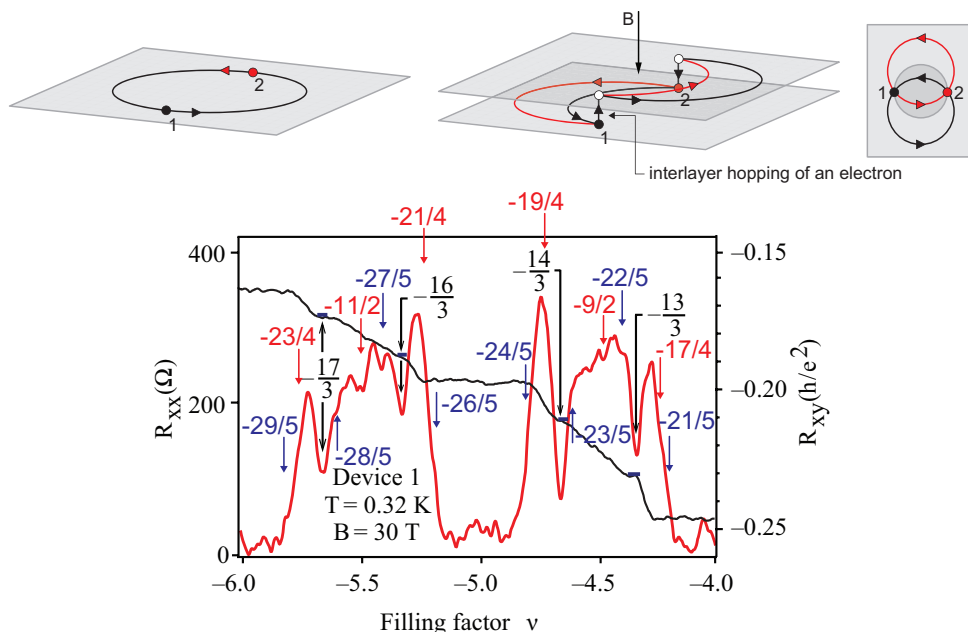


Fig. 8: Illustration of flux leakage for single-loop trajectory in bilayer and prediction, utilizing this effect, of all visible in experiment FQHE features [30] in bilayer-graphene for $n = 2$ (in two first subbands with $n = 2$ shown in the above figure)

The next topological oddness in bilayer is a possibility of hopping between layers of some part of a single-loop orbit [2, 8], cf. Fig. 7 – then the commensurability requirement is not applied to any layer, because it may happen that exchanging electrons along such a braid all time are in opposite layers. Then a dimension of a loop different than the corresponding to a nominal Landau index n is admissible (as shown in Fig. 7). Such a situation can be described as an effective leakage of flux, quantum by quantum. A complete analysis of such flux leakage gives simultaneous fitting of ca. 30 observed various features at $n = 2$ in bilayer graphene, when the interlayer leakage of flux is especially important [2] (Fig. 8). This perfect consistence with the experiment supports strongly the topological model²³. We propose also the development of this

²²The LLL is symmetrically divided between valence and conduction bands in graphene and by a lateral voltage one can shift the Fermi level between band holes and electrons, which provides a significant advantage over conventional GaAs Hall system.

²³Worth mentioning is the related discussion of the author with the experimental group of prof. D. Goldhaber-Gordon [30] by

experiment toward observation of FQHE in three-layer graphene where the trajectory homotopy will be still different but possible to be predicted upon the braid model.

2.10 Experimental verification of the braid model in bilayer graphene, the decisive experiment

The proposed by the author experiment with blockade of the interlayer hopping in bilayer graphene by application of a vertical voltage has been already performed with a different intention [79], but this experiment has confirmed forecasting of the proposed braid model. By partial blockade of interlayer hopping of electrons (in one direction) by a vertical voltage, the hopping of a trajectory is completely blocked. Trajectory hopping requires electron hopping in both directions (the trajectory must return because is closed), thus, an appropriate vertical electric field completely blocks interlayer trajectory hopping. In this way one can restore the monolayer topology in the bilayer system. This is a control over the homotopy by an external factor – the vertical voltage. One can remove by the vertical voltage all rich FQHE features in bilayer graphene induced by trajectory hopping. This has been observed in the experiment [79] (Fig. 9). This experimental demonstration of the topology change by simple application of the electrical field is a unique situation in correlated multiparticle systems.

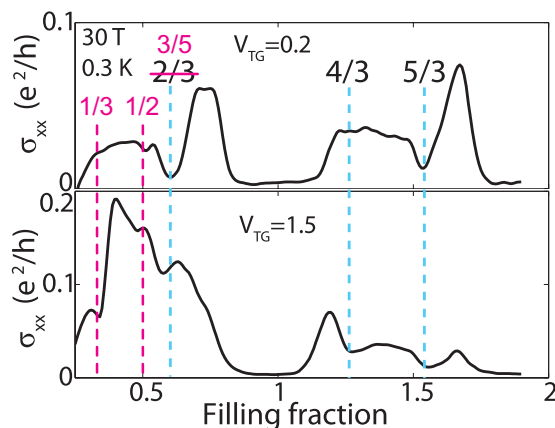


Fig. 9: By application of a vertical field which blocks the interlayer trajectory hopping one can change the trajectory homotopy from the specific to bilayer system to different one typical for monolayer graphene [2,8] – the experiment after [79], the state in $1/3$ instead of $1/2$ appears at larger voltage

The author proposes further development of this experiment [2,8] (addressed to groups of Maher, Dean and of Goldhaber-Gordon – is upon a discussion now) for bilayer graphene Hall samples with so-called 'open face' (i.e. with cut a window in upper layer of hBN for samples of bilayer graphene embedded in hBN). On such samples it has been obtained the most advanced observations of FQHE in bilayer graphene [30] (up to eight subband – which is the record score in whole Hall physics and follows from advances in sample preparation [30]). All the complicated and unusual observations of FQHE for $n = 2$ subbands have been explained by the braid model with inclusion of trajectory hopping, as described above. By the blockade of this hopping this rich FQHE behavior should be washed out. The 'open face' complicates, however fixing of the upper electrode defining the vertical voltage. It is a technical problem solely, moreover we discuss now with the mentioned experimental groups the feasibility for location of the upper electrode on the rim of the cut windows, because the homogeneity of the electric field produced by this electrode is not especially important. We expect that all visible features connected with described above leakage of the magnetic field

the occasion of the author action as the Referee of this publication in Nature Physics – this discussion is also published there

flux should disappear upon sufficiently strong voltage (of few V) and should be substituted by a different hierarchy typical for a monolayer Hall system for LL with $n = 2$, i.e., with filling fractions with denominator 5.

2.11 Generalization of the Bohr-Sommerfeld rule – mathematical rigorous verification of the braid model

The next our result [1] (it seems, with more fundamental significance exceeding the Hall system physics) is the generalization of quasiclassical Bohr-Sommerfeld rule onto the case of multiply connected space. The Bohr-Sommerfeld (B-S) rule refers quasiclassically to the case of 1D classical phase space (phase trajectory) in arbitrary shape 1D well with turning points on both barriers of the well²⁴. One can apply the B-S rule to a pair of components of kinematic momentum of a charged particle in 2D in the presence of perpendicular magnetic field B , when these components do not commute because of the field presence (e.g., taken in Landau gauge, $A = (0, Bx, 0)$) and this kinematic momentum components, $\hat{P}_x = -i\hbar\nabla_x$, $\hat{P}_y = -i\hbar\nabla_y - eBx$, create a pair of canonically conjugated variables, which can be treated as generalized position and momentum. Their 1D phase space in terms of kinematic momentum is 2D and corresponds to rotated by $\pi/2$ real position 2D space, which follows from also quasiclassical Lorentz force formula, $d\mathbf{P} = -e d\mathbf{r} \times \mathbf{B}$. The latter space can be in general multiply connected and indeed is such a space for multi-particle systems on a plane. In multiply connected space there are admissible (and sometimes obligatory) multiloop trajectories nonhomotopic with single-loop ones. Loops may occur only by one on the one-way traverse path between turning points and these loops can be counted by $k = 1, 2, \dots$, thus on the total closed phase-space cycle we have jointly $2k + 1$ loops.

The B-S integral for components of the kinematic momentum on the plane in the presence of magnetic field defines the size of the flux quantum of this field – it is $2k + 1$ times larger for k loops on a single one-way branch between turning points. This flux quantum has thus a larger surface at the same magnetic field than for loop-less one-way branch – this flux defines the size of multiloop cyclotron orbit. The sketched here derivation proves the size-increase of multiloop braids in 2D, which is utilized in commensurability analysis in the situation when single-loop braids are too short. The described above change of the size of flux quantum in multiply connected configuration space for 2D electrons in magnetic field is the reason of FQHE.

The generalization of the B-S rule [1] may have the significance not only for braid formalism but in all problems where the flux quantum is considered. For example, one could expect a fractional Josephson effect for a flux quantum for Cooper pairs, $(2k + 1)\frac{h}{2e}$ in multiply connected space instead of $\frac{h}{2e}$ in simply connected space. Unfortunately the odd homotopy is induced by the quantized magnetic field and its strength exceeds the critical field destroying superconductivity (perhaps fractional quantization by nonmagnetic Berry field might be here helpful).

Let us emphasize that the B-S rule and its application to quantization of the field flux is independent of interaction (as quasiclassical approach is not perturbative in interaction), thus holds at arbitrary strongly interacting systems. Hence, the B-S rule together with the topological its generalization to multiply connected space may be applied to strongly interacting electrons which are responsible for FQHE-state creation.

²⁴Quantum penetration into finite height wall causes 1/2 shift in the standard B-S rule. $\oint p dx = (n + \frac{1}{2})h$; the shift 1/2 is unimportant for topology question (for infinite vertical barriers 1/2 disappears).

2.12 Feynman path integral for kinetic nonstationary state and theoretical reproducing of the R_{xx} versus filling factor in the LLL (GaAs)

The next author result in the scientific achievement is an original development of the Feynman path integral [65, 66] onto situation of kinetic nonstationary quantum effect [1], when to the propagator must be included all trajectories corresponding to distinct allowed commensurability configurations at the same filling rate. Various commensurability patterns give different energies, but for a nonstationary state all energies must be included as the energy is not defined in such a quantum state. We have noticed that the number of different commensurability patterns at the same filling rate strongly depends on the filling rate ν . To different commensurability configurations at the same ν correspond distinct cyclotron braid subgroups defining distinct homotopy phases with distinct energies of correlated states. The lower energy defines the ground state. If an experiment is of kinetic type (e.g., the measurement of R_{xx}), then the corresponding quantum state should be characterized by Feynman integral including summation also over all admissible homotopy phases with various energies (as the energy is not determined in such state). Taking into account all possible commensurability configurations we performed a numerical simulation of relative value of Feynman path integral with varying ν . As the conductivity is proportional to the propagator, we found $R_{xx}(\nu)$ (inverted propagator). Surprisingly the numerically calculated curve appears to fit with the experimentally measured $R_{xx}(\nu)$ for GaAs in the LLL [1], cf. Fig. 4. This is for first time derivation of the longitudinal resistivity in Hall system. This result supports the braid model.

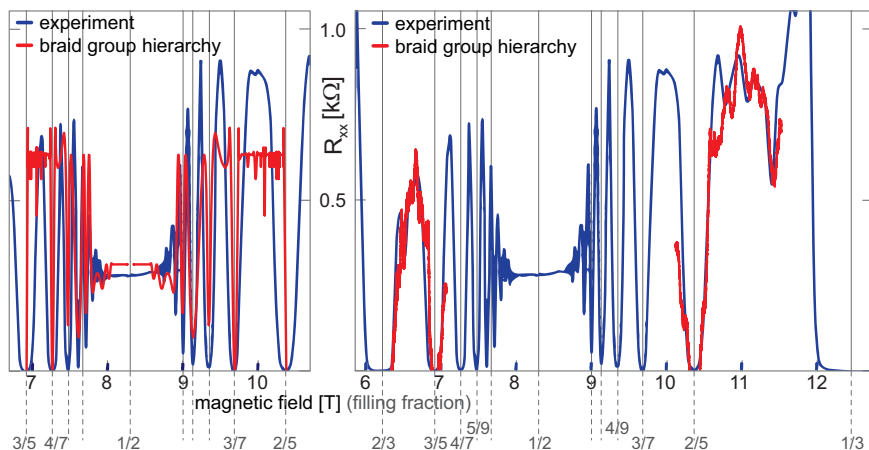


Fig. 10: Reproduction of $R_{xx}(\nu)$ in LLL (GaAs) by means of the generalized Feynman path integral for a nonstationary state [1], the theoretical curve – red, the experimental curve – blue

We noticed that on the curve $R_{xx}(\nu)$ for *enigmatic* states, i.e., the states for which are not admissible braid correlations with $x = 1$, R_{xx} does not reach zero in contrary to states defined by correlations with $x = 1$ (it is noticeable also a connection between the value of the depth of local minima of R_{xx} with the value of x) [1, 33]. It means that for such ν there is lower number of various admissible homotopy classes than for other ν with $x = 1$. Remembering that $x > 1$ indicates correlations of next-nearest neighbors for $q - 1$ first loops of q -loop trajectory (the last loop is controlled by $y \geq x$ in the general braid hierarchy) one can conclude that the absence of correlation of nearest neighbors results in the residual resistance.

2.13 Quantum simulation Monte-Carlo, novel visualization of correlation and symmetry for FQHE states

To the scientific achievement are included also our quantum simulations by Metropolis Monte-Carlo (MMC) method [69, 70] developed for trial wave functions defined for particular cyclotron subgroup homotopy pha-

ses. These wave functions are uniquely defined by the cyclotron braid subgroup generators in the LLL and their 1DURs (taking into account that any wave function for interacting system in the LLL must be holomorphic one [52]). The calculated by MMC method mean values of the energy very well agree with exact diagonalization of interaction in small systems and with measured activation energies (the activation energy is refined form the temperature dependence of resistivity drawn in the Arrhenius scale).

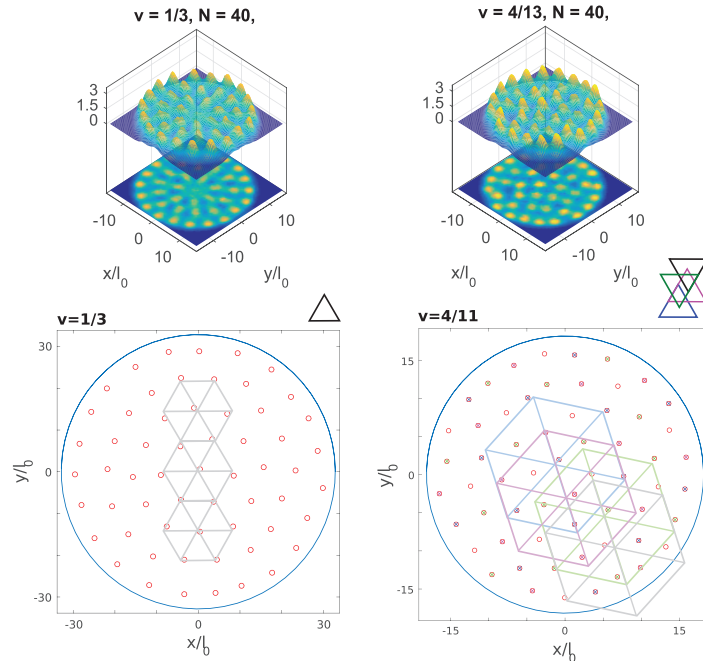


Fig. 11: Exemplary portrait of correlations (Pauli crystal) for $\nu = 1/3$ i $\nu = 4/11$ (*enigmatic*) calculated by specifically developed method of Metropolis Monte-Carlo-type simulation for braid group trial wave functions [13] – correlations of next nearest neighbors for $\nu = 4/11$ are noticeable

In the achievement it is presented numerical analysis (performed together with PhD student Patrycja Łydźba, the author is co-promotor of her thesis) for correlated states at various filling rates from FQHE hierarchy derived by the cyclotron braid group approach. The numerical simulations are done for relatively large number of electrons (up to 10^3) in geometry of circular plaquette (a continuation to the thermodynamic limit has been done similarly as in [69]). The correlations were also graphically visualized by determination of most probable positioning of particles in several-electron planar clusters. The virtual n -particle clusters (in analogy to detailed equilibrium in thermodynamics) were identified by quantum MMC-type simulation – determination of the most probable position of n -th electron, according to the trial multiparticle wave function, provided fixed positions of remaining $n-1$ electrons in the cluster. The latter have been found earlier by the same method for $n-1$ -particle cluster. The similar to inverted mathematical induction applied to n -particle cluster allow for determination of 'detailed distribution' of particles, being the portrait of correlations in the system [13]. These pictures found by us via development of the MMC method together with numerical annealing algorithm visualize the so-called Pauli virtual crystal. The correlation pictures reveal multiparticle symmetries characteristic to any state from the FQHE hierarchy. For comparison we analyzed also trial wave functions used in the CF model and obtained by a projection of wave functions from higher LLs onto the LLL in order to get a holomorphic function obligatory needed in LLL form non-holomorphic functions in higher LLs. The 'manual' method of removal poles is not uniquely defined and the projection onto LLL plays a role of variational procedure to optimize energy, but perturbs the symmetry in an uncontrolled manner. These perturbations are noticeable in the Pauli crystal-like portraits of correlations. In the method of braid

group we avoid these perturbations, and the symmetry of wave functions is uniquely defined by 1DURs of appropriate cyclotron braid subgroup generators together with decomposition of electrons into subsets nearest and next-nearest neighbors of various order defined in the general braid hierarchy for FQHE (in the LLL). The latter leads to unique form of the corresponding trial wave functions (similar to those determined earlier by Halperin [51]) and already holomorphic without a need of any projection onto the LLL.

2.14 Homotopy conditioning of IQHE, the role of interaction in IQHE

Considered by us cyclotron commensurability concerns rather surface-area of orbits than their radii. This commensurability bases on its archetype for IQHE – when the size (surface-area) of a cyclotron orbit equals to $\frac{h}{eB}$, i.e., it corresponds to a flux quantum $\frac{h}{e}$, and this surface-area is exactly equaled to $\frac{S}{N}$, where S is the sample surface and N is the number of electrons in the system (because for $\nu = 1$, $N = N_0 = \frac{BS_e}{h}$). From the latter condition it follows that the cyclotron orbits cannot be circular and cover the S surface, because it is impossible. Thus it is pointless to define cyclotron radius, but instead one must consider commensurability in terms of surfaces. The condition for IQHE, $\frac{S}{N} = \frac{S}{N_0} = \frac{h}{eB}$, is thus a fundamental pattern for all more complicated commensurabilities for interacting electrons.

Hence, one can notice that the IQHE state is also a correlated multiparticle state conditioned by the interaction as all FQHE states. The interaction is necessary to rigidly fix interparticle spacing obligatory needed for any commensurability and correlations. It is in opposition to popular in the literature opinion that IQHE is a single particle effect and can be understood only in single particle terms. This popular terminology 'single-particle' is linked with the fact that if the Jastrow polynomial transforms into the Vandermonde polynomial in the Laughlin function at transition from FQHE state into IQHE state, then the true wave function for correlated, strongly interacting system as is IQHE state has formally the same form as for non-interacting gas of 2D electrons. This coincidence is the result of the cyclotron braid group symmetry and its 1DUR for $\nu = 1$ in the interacting system, and on the other hand the same braid group (not cyclotron one, however, as not resulted from any commensurability in gas) – sole braid group available in gas (cyclotron braids subgroups cannot be defined in the gas). The Hamiltonians of both different system, with and without interaction are, however, different, which results in distinct energies for the same-looking wave function. For the gas this energy is zero counted from the zeroth Landau level but in the interacting system the energy is negative in the same scale, caused by the sum of energy of jellium-jellium, jellium-electron, electron-electron interactions (from our MMC simulations we estimated this energy as $-0.58 \frac{e^2}{4\pi\epsilon_0\epsilon l_B}$ per particle and surface unit l_B^2 [8]). The same has been observed by Haldane and expressed in terms of so-called pseudopotential of interaction in Hall system – matrix elements of interaction in the basis of angular momenta of interacting electron pair [52]).

In gas the commensurability loses its sense because distance between particles can be arbitrary small or large (in thermodynamical limit) and none constraints are imposed on the pure braid group. The resulting fermions, bosons or anyons are, however, *not correlated*. The complete filling of the LLL does not mean IQHE – the latter is the correlated state. Even though it is possible to completely fill the LLL with the electron gas, similarly as higher LLs – these states are not correlated and are frequently observed in many systems (metals, semiconductors) at magnetic field, when interaction is small, i.e., the correlations induced by this interaction is washed out by a temperature chaos. The correlated states in 2D occur at ultra-small temperature and for $n \leq 2$ as for higher n the lowering with n correlation energy is dominated by the thermal chaos, kT . All FQHE states as well as IQHE state are correlated and therefore so much fragile. Filling of LLs including LLL can take place at larger temperatures as well, but do not correspond then to IQHE.

The correlated FQHE and IQHE states are not quantum phases with any local order parameter (linked with the mass operator [73]), they are collective strongly correlated states of the whole system with correlations imposed by cyclotron braid subgroup commensurability. These states can be called as homotopy phases and they define a specific class of quantum phases without any order parameter. The quantum phase transition between these homotopy phases can undergo at $T=0$ due to step-wise change of the commensurability patterns induced by the magnetic field shift and resulting in different energies.

One can notice that the concept of the cyclotron braid commensurability with interacting electron distribution is universal. Despite different microscopic material realizations the resulted hierarchy of fillings is the same in GaAs or graphene and even in fractional topological Chern insulator [37, 38]. In the latter case, in continuation of the Haldane model [49], one deals with integral or fractional Hall-type effects though without uniform magnetic field and without Landau levels. Quantum Hall effects in these materials correspond to commensurability of electron distribution with different than cyclotron orbits. The role of cyclotron orbits is taken here by Berry phase orbits [80] corresponding to traversing of the unite cell. Triple-loop enhances the orbit size which fits to $1/3$ electron filling counted per the lattice node – and this is observed in numerical experiments [37, 38].

2.15 Phase diagram for competition of superfluidity of indirect excitons and IQHE-reentrant in twin Hall systems with insulating barrier and for complementary filling of layers

An employment of described above observations and developed methods in Hall systems (and the possibility of calculation of quantum mean energy of interaction for large number of electrons by MMC method) has been demonstrated in the following author papers [3, 4] for analysis of intensively currently studied new experimental configuration of Hall systems [81–83], namely of a pair of parallel Hall systems separated by an insulating barrier thick enough to prevent interlayer tunneling of electrons but allowing still strong Coulomb interaction across the barrier. For Hall GaAs such systems there are applied insulating barriers GaAlAs with thickness $d > 1.4l_B$, where $l_B = \sqrt{\frac{\hbar}{eB}}$ is the magnetic length (for $B = 10\text{T}$ l_B equals to ca. 10 nm) and for graphene Hall layers the insulating layer is hBN layer (hexagonal boron nitride) with better insulating properties than GaAlAs and blocking of electron tunneling even for $d \sim 0.5l_B$ (both insulators are accommodated in crystalline structure to materials of Hall systems to avoid disorder). Advances in preparation of multilayer graphene hetero-structures (especially with bilayer graphene as Hall layers) considerably accelerates the related experiment in 2016 – 2017 [82, 83]. The goal of these experiments is especially ambitious, because assumes and the system actually realizes superfluid condensate of excitons (longly searched in whole condensed matter) [84]. The superfluid of Bose-Einstein condensate forms of pairs of Landau electrons and holes from reciprocal Hall layers and occupying complementary filled layers, $\nu_{top} + \nu_{bot} = 1$, i.e., of electrons(holes) and holes(electrons) oppositely located in *top* and *bottom* layers.

The phenomenon of superfluidity of separated oppositely charged carriers paired across the insulating layer (and thus creating a stable exciton) is intriguing and has been observed experimentally via (*drag*) of interlayer coupled carriers and via so-called (*counterflow*), the latter considered as an experimental evidence of superfluidity of exciton condensate. We have originally applied and developed a two-component Bogolubov-type model [4] for superfluid excitons. In comparison to previous models we have proposed the modification – the two component exciton system (in former papers it has been developed only the single-component model being a direct continuation of hypothetical previously studied (unstable) exciton systems in a single layer, when the exciton polarization has been not important and not defined [85, 86]). If, however, both layers are spatially separated, the polarization of indirect-interlayer excitons, (\pm) or (\mp), starts to be

important and, in our opinion [3,4], plays a crucial role for stability of the superfluid condensate. Accounting for of the exciton polarization made the model more realistic. In the conventional Bogolubov model it is seen that the superfluidity requires repulsion of bosons in the condensate. Excitons are not indeed bosons, because are created by pairs of fermions in exclusively single states. Nevertheless, the Bose-Einstein condensation is available here because all Landau electrons and holes (and thus excitons) have the same energy by virtue of massive degeneracy of Landau levels [85] – these excitons create Bose-Einstein condensate which is superfluid provided that excitons repulse themselves. Just this repulsion is linked with exciton polarization and their distribution which we propose in our paper [3,4]. In our model we originally propose a specific structure of complementary in both layer alternately ordered stripes (accommodated to opposite polarization of both components of the system) defined in the k space (where k enumerates states of electrons and holes in Landau subbands, at Landau gauge of magnetic field); we show that the eventual stripe structure is gauge independent and assures an optimal repulsion of excitons and stability of both superfluid phases in the twin Hall system. With this ordering and the superfluid coherence competes, however, the homotopy correlated IQHE-*reentrant* state, which we originally proposed. This quantum integer Hall ordering also requires striping as nominal filling of both layers is fractional. This striping is optimized in a different manner than k striping due to different energy gain in correlated phase versus coherent superfluid phase. The former we accounted by application of the MMC numerical simulation [69] for estimation of the mean value of energy according IQH-reentrant multiparticle wave function in striped structure²⁵. The stripe structure is here essential both for IQH-reentrant phase (as it occurs at fractional fillings in both layers – thus may be only of reentrant type due to striping with stripes filled up to local $\nu = 1$) and for exciton superfluid phase because of required k striping assuring repulsion of excitons and in both polarized exciton components.

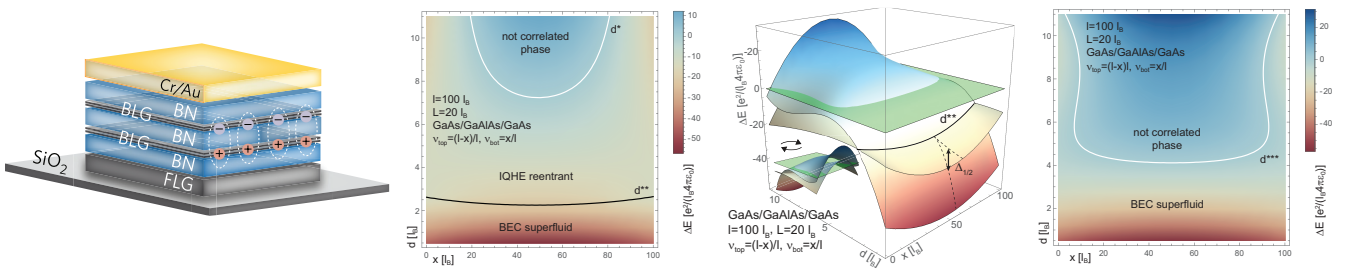


Fig. 12: Exemplary phase diagrams for competition of superfluid Bose-Einstein condensate of indirect excitons and IQHE-reentrant for experimental configurations *counterflow* (fourth panel) and *drag* (second panel); third panel – hyperplanes of energies of competing phases in drag configuration, first panel – schematic view on bilayer-graphene/hBN/bilayer-graphene setup [3,4]

In the paper [4] author presented quantum simulation of MMC type of a complex twin Hall system with two 2D layers separated by an insulating barrier thin enough to allow for coupling of holes and electrons from opposite Hall layers and for the creation of indirect excitons at complementary filling of both layers, $\nu_{top} + \nu_{bot} = 1$ (subscript *top(bot)* refers to top(bottom) layer). The model founds a link to the experimentally demonstrated [82, 83] competition of superfluidity of Bose-Einstein condensate of indirect excitons and of IQHE in b-graphene/hBN/b-graphene (and formerly in GaAs/GaAlAs/GaAs described earlier in the series of mostly by Eisenstein papers listed in [3,4]). The theory was not completed previously, especially with respect to a phase diagram of these systems. We have filled this gap and have provided the model for

²⁵The method utilizes a random walk in the multiparticle configuration space with positive feedback guaranteeing probability enhancement according to the wave function. The resulting distribution of particles after ca. 10^8 steps of a walk, gives the 'detailed distribution' allowing the energy assessment. Averaging over the large number of detailed distributions (of order of 10^8) defines the searched quantum mean value of energy with very high accuracy.

competition of various phases – superfluidity of excitons and IQHE taking advantage of our original concept of striping resulting in the phase diagram [3,4]. Except of the idea of striping in the system we proposed also a generalization of former model of superfluidity of indirect excitons toward two component (distinguished with polarization) Bogolubov model of superfluid excitons. Two component model fit conveniently with our concept of striping and occurs optimal for coupling of electron(hole) with reciprocal hole(electron) but in specially accommodated Landau states one in front of another across the barrier. We have performed a complex simulation MMC of the total system which resulted in phase diagrams for competition of both correlated phases versus imbalanced complementary layer fillings and the barrier thickness (as for example is illustrated in Fig. 12) The phase diagrams we found in two distinct experimental configurations [87]: counterflow and drag. These diagrams, for the first time found theoretically, appears to be consistent with experimental observations in GaAs/GaAlAs/GaAs and in b-graphene/hBN/b-graphene. Agreement is even quantitative with respect to position and shape of transition curves and with respect to the activation energy of particular phases. In GaAs/GaAlAs/GaAs we explained and removed the former two-order-large discrepancy between the experimental value of the activation energy and its former estimation without taking into account of the FQHE-reentrant phase. We have also explained [4] two puzzling experimental observations from 2017 in b-graphene/hBN/b-graphene:

1. An absence of a counterflow signal, i.e., disappearance of superfluidity in states in b-graphene LLL with $n = 1$, despite superfluidity presence (and counterflow presence) in states with $n = 0$ or $n = 2$ [82]. We found [4] the reason of it in four-fold lower repulsion of electrons(holes) in stripes for $n = 1$ in comparison to $n = 0$ or $n = 2$ (for $n = 1$ disappears a central peak in local density due to first Hermite polynomial in this level in contrary to second and zeroth Hermite polynomials; it is visible at any gauge). For lower repulsion the stability of superfluid of excitons falls down (according to Bogolubov model, we applied) which is observed in the experiment [83] via disappearance of counterflow signal for $n = 1$.
2. The second puzzling effect is the absence of the Hall response in drag configuration of the total system filled with valence band holes with filling scheme $(\nu_{top} = -\frac{1}{2}, \nu_{bot} = -\frac{1}{2})$ in b-graphene/hBN/b-graphene, despite sharply visible such a response at mirrorous filling in conduction band $(\frac{1}{2}, \frac{1}{2})$ in the same sample (filling is controlled by a lateral voltage). In our stripe model such a behavior is understandable via oddness of stripes with band holes and simultaneously Landau holes being in fact empty jellium stripes completely Hall passive in contrary to electron mirrorous stripes [4]. This (including further details presented in [4]) well agrees with the experiment [82,83] and is also confirmed by a return of Hall response if valence-band holes acquire additional degrees of freedom (as at e.g., filling of b-graphene/hBN/b-graphene $(-\frac{3}{2}, -\frac{1}{2})$ with $\nu_{total} = \nu_{bot} + \nu_{top} = -2$).

Moreover, in the paper [3] it has been solved a problem from pioneering observation of odd FQHE in GaAs bilayer Hall system but with interlayer tunneling of electrons admitted. In the experiment [88,89] has been observed FQHE states at unexpected fillings $1/4$ and $1/2$ of both layers, which was not explained by a conventional theory. However, the application of a homotopy braid model occurs helpful in identification of all observed FQHE details in the bilayer system [3]. This contributes a long discussion on synergy and competition between tunneling and interaction across a barrier in Hall bilayer in organization of correlated quantum states.

Comparison of two-layer Hall system configurations: 1) bilayer system with hopping of electrons between layers (like bilayer-graphene), 2) twin 2D layer Hall systems with insulating barrier between blocking tunneling of electrons, reveals a different physics in both cases, as described by the author in presented

achievement. The 1) case is described by the homotopy model of bilayer with characteristic FQHE hierarchy different than in monolayer – the hallmark here is the FQHE state at $\nu = 1/2$ for whole system (i.e., $1/4$ per layer)²⁶. For 2) one can encounter superfluidity for $1/2$ filling of each layers (or other complementary filling), which may compete (depending of barrier thickness) with IQHE-reentrant – this is, however, not the same as filling of 1) type bilayer $1/2$ per layer (the latter would give for total bilayer $\nu = 1$ and ordinary IQHE in it, which is not observed in 2)). It is interesting to note that since 90. there are not well understood as of yet pioneering experiments with bilayer of GaAs [88, 89] mixing 1) and 2) situations. Developed upon the achievement theories addressed to 1) and to 2) as described above, allow to re-discuss these experiments [3] (it is currently developed by the author in collaboration and discussion with Z. Papić and A. MacDonald and F. Peeters).

2.16 Summary

The model of quantum homotopy phases developed and demonstrated in applications, seems to contribute to the theory and current understanding of the Hall physics. This model:

- is mathematically rigorous – exploits the well developed in algebraic topology formalism of homotopy π_1 group, in particular of braid groups, and cyclotron braid subgroups originally defined via introduction of a commensurability notion to the braid group structure,
- defines quantum hierarchy for FQHE on the basis of Feynman path integral for multiparticle interacting systems in 2D manifold with especially rich braid group including cyclotron braid subgroups,
- is universal, can be applied to the LLL and also to higher LLs in conventional 2DEG GaAs upon a magnetic field as well as to graphene monolayer and bilayer in magnetic field or even to fractional topological Chern insulators with magnetic field substituted by the Berry field (without LLs and filling fraction counted per elementary cell)
- defines a complete FQHE hierarchy, Hall metal hierarchy and hierarchy of paired states in consistence with available at present experimental data (ca. 150 features of hierarchy in 2DEG GaAs and in graphene),
- explains a controversial anomalous FQHE in bilayer graphene,
- explains the physical foundation of states beyond a conventional CF hierarchy in the LLL (called in the literature as enigmatic states and observed in 2DEG GaAs),
- elucidates the phenomenological model of CFs and precisely defines the range of its applicability; elucidates the structure of multicomponent Halperin states via braid correlations of various orders next-nearest neighbor subsets of electrons,
- provides a rigorous method for definition of trial wave functions and precisely determines their symmetry in terms of 1DURs of cyclotron braid subgroups (in contrary to projection from higher LLs onto the LLL in the model of CFs, perturbing the symmetry in an uncontrolled manner),
- provides states (trial wave functions) for fillings from hierarchy with very good consistence of energies with exact diagonalization of small models and with activation energies experimentally observed,

²⁶Let us notice that if one considers the bilayer of conventional semiconductor Hall 2DEG (GaAs) layers then the state at $\nu = 1/2$ must realize as FQHE because in GaAs we have not the $n = 1$ state in the LLL subband in contrary to bilayer graphene allowing in b-graphene to dismiss $1/2$ FQHE state when is filled first $n = 1$ subband before $n = 0$ subband.

- allows for a development of the Feynman integral for various configurations of cyclotron commensurability with particle separation including multi-loop orbits and for nonstationary case for the path integral including homotopy patterns with various energies,
- reproduces, for the first time, the experimental complicated curve $R_{xx}(\nu)$ for the LLL (GaAs),
- defines the generalization of Bohr-Sommerfeld rule for multiply connected spaces, which allows for identification (independently of interaction) of generalized magnetic field flux quantum in a multiply connected space (different than $\frac{h}{e}$ correct in the simply connected space),
- allows for quantitative description of IQHE-reentrant and finding, for the first time, of the phase diagram for competition of superfluidity of excitons and IQHE-reentrant in twin Hall systems with insulating barrier, in good quantitative consistence with experiment in GaAs/GaAlAs/GaAs and in b-graphene/hBN/b-graphene,
- allow for understanding of synergy and competition of interlayer tunneling and interaction in bilayer Hall systems
- allows for a visualization of braid correlations in FQHE states (via Pauli virtual crystal).

From the above listed range of presented topological model and of its applications one can notice its utility for better insight into conditioning of FQHE and for explanation or formerly applied models of CFs and of Halperin multicomponent functions. Strongly convincing is a very good consistence with experiment with regard of all known at present FQHE hierarchy details in various materials. Especially supporting is the explanation of the anomalous FQHE in bilayer graphene (of all observed ca. 30 features up to eight LL subband and being completely out of reach for CF model) and the original reproducing of longitudinal resistivity versus filling fraction in the LLL GaAs via generalization of the Feynman path integral onto non-stationary case. Important is also invoking in the developed model to rigorous mathematical results, with emphasizing here of the decisive character of the generalization of Bohr-Sommerfeld rule for multiply connected spaces, the formalism of cyclotron subgroups and their representations and, on the other hand, invoking to also decisive experiment demonstrating the specific to braid theory change of the homotopy from bilayer to monolayer one by blockade of interlayer hopping of electrons in bilayer graphene or in GaAs bilayer.

The proposed homotopy cyclotron braid model successfully explains all details of FQHE hierarchy experimentally noticed so far. It is especially important with regard to recent observations of controversial FQHE features in graphene monolayer and bilayer and in higher LLs in all Hall materials, where the conventional models are insufficient. The new approach unravels also the essence of the heuristic CF model as limited to only nearest neighbor commensurabilities (i.e., the limit $x = 1$ in the commensurability condition as described above) and identifies situations when CF are not applicable (as for single-loop FQHE states in higher LLs or trajectory hopping in bilayer graphene or bilayer GaAs). It can be added that reducing of the applicability range of CF model causes a conservative attitude with regard to any corrections of the conventional CF model widely spread since over 25 years, which leads to difficulties with publication of a new theory in journals being upon influence of CF followers²⁷. It is, however, clear that CFs are not any quasiparticles, i.e., they are not electrons dressed with interaction as it was originally suggested [40], but are rather a convenient effective illustration of additional braid loops by artificial auxiliary field flux quanta pinned to electrons (one quantum – one loop in the cyclotron orbit). CFs are not a local result of the interaction solely but are a

²⁷Especially in PRL where Jainendra K. Jain was EBM and Samindranath Mitra is Ed. of QHE branch, and in PRB where Hari Dahal is Ed. of QHE branch, both followers of Jain's CF model.

pictorial effective representation of a nonlocal commensurability pattern, moreover, in its simplest case, in more complicated ones the CF picture is, however, irrelevant. In 2D Hall systems the interaction does not play the role of a local 'quasiparticle dress'. Recently, the new FQHE topology-based nonlocal theory causes a growing interest of specialists, e.g., of A. MacDonald, Z. Papić, D. Goldhaber-Gordon, D. Haldane, F. Peeters.

The braid group homotopy model explains the inapplicability of CFs in higher LLs and their inconsistency with experiment in bilayer graphene. The cyclotron braid model recognized the role of electron interaction generating correlations but upon the specific homotopy-type patterns of quantization in planar multiply connected system, which determines various homotopy phases at various filling rates by cyclotron commensurability in 2D. This is not a local phenomenon like dressing of bare electrons with interaction, the concept of Landau-type quasiparticle is here not applicable²⁸. The Feynman path formulation for many particle systems clarifies a two-fold channel of interaction entrance – via the commensurability of trajectories possible only provided the interaction is present, and via Lagrangian in the action. Both channels of interaction entrance are also involved in the exact diagonalization of small models, though in an implicit manner (the commensurability enters the exact diagonalization via rigidly kept particle number, sample surface and magnetic field value). This implicit character causes some misleading opinion that the differences of FQHE hierarchy in higher LLs or in graphene are induced by single-particle Landau wave function shapes varying with changing of Landau index n and reproducing microscopic material specifics (like in graphene). This is not true – the FQHE hierarchy is universally conditioned by homotopy constraints and not by dynamic details, the latter (including shapes of single-particle states) decide only on values of activation energies for particular filling rates selected, however, by the topological commensurability condition for repulsing charged particles in 2D upon perpendicular magnetic field.

The cyclotron braid model defines the FQHE hierarchy more completely than the CF or Halperin models and does not use any artificial phenomenological assumptions, but rather explains an essence of auxiliary elements in other models. The advantage of the braid model is its rigorous mathematical formulation and a full agreement with experiment in all materials revealing QFHE-type correlations. The model has been verified by decisive experiment in bilayer graphene with changing the homotopy by vertical voltage and is essentially supported by an accurate and formal generalization of Bohr-Sommerfeld rule in multiply connected spaces, which defines the related magnetic field flux quantum (different than $\frac{h}{e}$, being correct in simply connected space). Author publications included to the scientific achievement cycle [1–16] describe step-by-step the construction of the final homotopy cyclotron braid model formulation and its applications, the most advanced and essential publications are [1–5, 7, 9].

Listing of most important results with reference to publications included to the presented scientific achievement:

1. generalization of Bohr-Sommerfeld rule for the case of multiply connected space [1]
2. introduction of cyclotron commensurability to the structure of the braid group [2, 8, 16]
3. determination of the general form for magnetic field flux quantum in multiply connected space with nontrivial cyclotron braid subgroup [1]
4. introduction of the notion of the homotopy phase describing correlations in 2D and of the homotopy quantum phase transition [1, 2, 7]
5. generalization of the Feynman path integral for different homotopy phases [9, 12, 16]
6. derivation of the complete FQHE hierarchy in the LLL (GaAs) consistent with experiments including

²⁸For example, in 3D FQHE is not observable despite the interaction.

- enigmatic* hierarchy elements [5, 8, 14, 15]
7. definition of trial wave functions for states from identified hierarchy and estimation (MMC method) of their energies in agreement with exact diagonalization of small models and measured activation energies [2, 8, 15]
 8. providing of explanation of the essence of CF model and precise identification of limits of its applicability [1, 2, 16]
 9. introduction, for the first time, of a new class of FQHE states (single-loop ones) in higher LLs [11]
 10. illustration of symmetry perturbations in due of projection onto the LLL in CF model; introduction of homotopy correlation portrait by the Pauli virtual crystal [13]
 11. clarification of the reason for universal manifestations in various materials of FQHE hierarchy (GaAs, graphene, fractional topological Chern insulator) [1, 2, 5, 8]
 12. identification and explanation of the reason of high mobility requirement for organization of FQHE [10]
 13. derivation of general Hall metal hierarchy and of paired states (GaAs, graphene, in the LLL and in higher LLs) [2, 5, 7, 13, 15]
 14. explanation of unconventional FQHE hierarchy observed in graphene monolayer $n = 1$ [5, 6, 14]
 15. explanation of anomalous hierarchy of FQHE in graphene bilayer, $n = 0, 1, 2$ [2, 6]
 16. generalization of Feynman path integral onto non-stationary state and theoretical derivation, for the first time, of the function $R_{xx}(\nu)$ for LLL GaAs [1]
 17. introduction of two-component Bogolubov model of superfluidity of indirect excitons in complementary filled twin Hall systems separated by dielectric barrier and of the stripe model in Landau k space [4]
 18. identification (for the first time) of the phase diagram for competition of superfluidity of excitons and IQH-reentrant state in twin Hall systems [3, 4]
 19. clarifying of experimentally observed puzzling absence of counterflow response for $n = 1$ LLL states in b-graphene and absence of Hall response for complementary filling $(-0.5, -0.5)$ of b-graphene/hBN/b-graphene [4]
 20. explanation of odd FQHE states observed in 90. in of closely adjacent bilayer GaAs at fillings $1/4$ and $1/2$ of both layers [3]

Literatura

- [1] J. Jacak, “Application of the path integral quantization to indistinguishable particle systems topologically confined by a magnetic field,” *Phys. Rev. A* **97**, p. 012108, 2018.
- [2] J. Jacak, “Unconventional fractional quantum Hall effect in bilayer graphene,” *Sci. Rep.* **7**, p. 8720, 2017.
- [3] J. Jacak, “Superfluidity of indirect excitons vs quantum Hall correlation in double Hall systems: different types of physical mechanisms of correlation organization in Hall bilayers,” *Phys. Lett. A*, 2018. doi.org/10.1016/j.physleta.2018.07.007.
- [4] J. Jacak, “Phase diagrams for superfluidity of indirect excitons in double Hall systems GaAs/GaAlAs/GaAs and bilayer-graphene/hBN/bilayer-graphene,” *Europhys. Lett.* **123**, p. 16001, 2018. (+ Supplementary Materials 1-11), doi.10.1209/0295-5075/123/16001.
- [5] P. Łydźba, L. Jacak, and J. Jacak, “Hierarchy of fillings for the FQHE in monolayer graphene,” *Scientific Reports* **5**, p. 14287, 2015.
- [6] J. Jacak and L. Jacak, “Unconventional fqhe in monolayer and in bilayer graphene,” *Science and Technology of Advanced Materials* **17**, p. 149, 2016.
- [7] J. Jacak and L. Jacak, “Commensurability condition and hierarchy of fillings for fqhe in higher landau levels in conventional 2deg systems and in graphene—monolayer and bilayer,” *Phys. Scr.* **91**, p. 015802, 2016.
- [8] J. Jacak, “Unconventional fractional quantum Hall effect in bilayer graphene,” *Sci. Rep. Supplementary Information* **7**, pp. 8720(1–14), 2017.

- [9] J. Jacak and L. Jacak, “Explanation of $\nu=-1/2$ fractional quantum hall state in bilayer graphene,” *Proc. R. Soc. A* **472**, p. 20150330, 2016.
- [10] J. Jacak and L. Jacak, “On triggering role of carrier mobility for Laughlin state organization,” *JETP Letters* **98**, p. 776, 2013.
- [11] J. Jacak and L. Jacak, “The commensurability condition and fractional quantum hall effect hierarchy in higher Landau levels,” *JETP Letters* **102**, pp. 19—25, 2015.
- [12] P. Łydźba and J. Jacak, “Topological origin and not purely antisymmetric wave functions of many-body states in the lowest Landau level,” *Proc. Royal Soc. A* **473**, p. 20160758, 2017.
- [13] P. Łydźba and J. Jacak, “Identifying particle correlations in quantum hall regime,” *Annalen der Phys.* **530**, p. 1700221, 2018.
- [14] J. Jacak and L. Jacak, “Difference in hierarchy of FQHE between monolayer and bilayer graphene,” *Phys. Lett. A* **379**, p. 2130, 2015.
- [15] J. Jacak, P. Łydźba, and L. Jacak, “Topological approach to quantum Hall effects and its important applications: higher Landau levels, graphene and its bilayer,” *Eur. Phys. J. B* **90**, p. 90, 2017.
- [16] J. Jacak, R. Gonczarek, L. Jacak, and I. Józwiak, *Application of Braid Groups in 2D Hall System Physics: Composite Fermion Structure*, World Scientific, Singapore, 2012.
- [17] J. Jacak, *Topological approach to Fractional Quantum Hall Effect in monolayer and bilayer graphene*, ch. Handbook on the Graphene Materials. Advanced Materials Book Series, Wiley, 2018.
- [18] J. Jacak, I. Józwiak, L. Jacak, and K. Wieczorek, “Cyclotron braid group structure for composite fermions,” *J. Phys. Cond. Matter* **22**, p. 355602, 2010.
- [19] J. Jacak, P. Łydźba, and L. Jacak, “Homotopy approach to fractional quantum Hall effect,” *Appl. Math.* **6**, p. 345, 2015.
- [20] J. Jacak and L. Jacak, “The triggering role of carrier mobility in the fractional quantum Hall effect formation—an evidence in graphene,” *J. Mod. Phys.* **4**, p. 1591, 2013. invited to Special Issue: Topological Insulators and Low Dimensional Quantum Physics.
- [21] J. Jacak, P. Łydźba, and L. Jacak, “Fractional quantum Hall effect revisited,” *Physica B* **475**, p. 122, 2015.
- [22] J. J. P. Łydźba, “Many-body wave functions for correlated systems in magnetic fields: Monte Carlo simulations in the lowest Landau level,” *J. Phys. Cond. Matter*, 2018. (in press).
- [23] J. Jacak and L. Jacak, “Recovery of Laughlin correlations with cyclotron braids,” *Europhysics Lett.* **92**, p. 60002, 2010.
- [24] J. Jacak, I. Józwiak, and L. Jacak, “Composite fermions in braid group terms,” *Open Sys. and Inf. Dyn.* **17**, p. 1, 2010.
- [25] J. Jacak, “Bilayer graphene as the material for study of the unconventional fractional quantum Hall effect,” in *Graphene Materials: Structure, Properties and Modifications*, G. Z. Kyzas, ed., ch. 3, pp. 49–76, INTECH, 2017.
- [26] J. Jacak, I. Józwiak, and L. Jacak, “New implementation of composite fermions in terms of subgroups of a braid group,” *Phys. Lett. A* **374**, p. 346, 2009.
- [27] J. Jacak, I. Józwiak, L. Jacak, and K. Wieczorek, “Cyclotron braid group approach to Laughlin correlations,” *Adv. Theor. Math. Phys.* **15**, p. 449, 2011.
- [28] J. Jacak, R. Gonczarek, L. Jacak, and I. Józwiak, “Explanation of composite fermion structure in fractional quantum Hall systems,” *Int. J. Mod. Phys. B* **26**, pp. 1230011–1–60, 2012.
- [29] P. Łydźba and J. Jacak, “Ultra-quantum 2d materials: Graphene, bilayer graphene, and other Hall systems—new non-local quantum theory of Hall physics,” in *Recent Advances in Graphene Research*, P. Nayak, ed., ch. 1, pp. 3–29, INTECH, 2016.
- [30] G. Diankov, C.-T. Liang, F. Amet, P. Gallagher, M. Lee, A. J. Bestwick, K. Tharratt, W. Coniglio, J. Jaroszynski, K. Watanabe, T. Taniguchi, and D. Goldhaber-Gordon, “Robust fractional quantum hall effect in the $n=2$ landau level in bilayer graphene,” *Nature Comm.* **7**, p. 13908, 2016.
- [31] D. C. Tsui, H. L. Störmer, and A. C. Gossard, “Two-dimensional magnetotransport in the extreme quantum limit,” *Phys. Rev. Lett.* **48**, p. 1559, 1982.
- [32] R. B. Laughlin, “Anomalous quantum Hall effect: an incompressible quantum fluid with fractionally charged excitations,” *Phys. Rev. Lett.* **50**, p. 1395, 1983.
- [33] W. Pan, H. L. Störmer, D. C. Tsui, L. N. Pfeiffer, K. W. Baldwin, and K. W. West, “Fractional quantum Hall effect of composite fermions,” *Phys. Rev. Lett.* **90**, p. 016801, 2003.

- [34] F. Amet, A. J. Bestwick, J. R. Williams, L. Balicas, K. Watanabe, T. Taniguchi, and D. Goldhaber-Gordon, “Composite fermions and broken symmetries in graphene,” *Nat. Commun.* **6**(6838), 2015.
- [35] D. K. Ki, V. I. Falko, D. A. Abanin, and A. Morpurgo, “Observation of even denominator fractional quantum Hall effect in suspended bilayer graphene,” *Nano Lett.* **14**, p. 2135, 2014.
- [36] F. D. M. Haldane, “Model of quantum Hall effect without Landau levels: condensed matter realization of the ‘parity anomaly’,” *Phys. Rev. Lett.* **61**, p. 2015, 1988.
- [37] D. N. Sheng, Z.-C. Gu, K. Sun, and L. Sheng, “Fractional quantum Hall effect in the absence of Landau levels,” *Nature Comm.* **2**, p. 389, 2011.
- [38] T. Liu, C. Repellin, B. A. Bernevig, and N. Regnault, “Fractional Chern insulators beyond Laughlin states,” *Phys. Rev. B* **87**, p. 205136, 2013.
- [39] J. K. Jain, “Composite-fermion approach for the fractional quantum Hall effect,” *Phys. Rev. Lett.* **63**, p. 199, 1989.
- [40] J. K. Jain, *Composite Fermions*, Cambridge UP, Cambridge, 2007.
- [41] Y. Aharonov and D. Bohm, “Significance of electromagnetic potentials in quantum theory,” *Phys. Rev.* **115**, p. 485, 1959.
- [42] J. P. Eisenstein, M. P. Lilly, K. B. Cooper, L. N. Pfeiffer, and K. W. West, “New physics in high Landau levels,” *Physica E* **6**, p. 29, 2000.
- [43] W. Pan, K. W. Baldwin, K. W. West, L. N. Pfeiffer, and D. C. Tsui, “Fractional quantum hall effect at landau level filling $4/11$,” *Phys. Rev. B* **91**, p. 041301(R), 2015.
- [44] N. Samkharadze, I. Arnold, L. N. Pfeiffer, K. W. West, and G. A. Csáthy, “Observation of incompressibility at $\nu = 4/11$ and $\nu = 5/13$,” *Phys. Rev. B* **91**, p. 081109, 2015.
- [45] A. Kumar, G. A. Csáthy, M. J. Manfra, L. N. Pfeiffer, and K. W. West, “Nonconventional odd-denominator fractional quantum hall states in the second landau level,” *Phys. Rev. Lett.* **105**, p. 246808, 2010.
- [46] C. R. Dean, A. F. Young, P. Cadden-Zimansky, L. Wang, H. Ren, K. Watanabe, T. Taniguchi, P. Kim, J. Hone, and K. L. Shepard, “Multicomponent fractional quantum Hall effect in graphene,” *Nature Physics* **7**, p. 693, 2011.
- [47] B. E. Feldman, B. Krauss, J. H. Smet, and A. Yacoby, “Unconventional sequence of fractional quantum Hall states in suspended graphene,” *Science* **337**, p. 1196, 2012.
- [48] A. Kou, B. E. Feldman, A. J. Levin, B. I. Halperin, K. Watanabe, T. Taniguchi, and A. Yacoby, “Electron-hole asymmetric integer and fractional quantum hall effect in bilayer graphene,” *Science* **345**(6192), pp. 55–57, 2014.
- [49] F. D. M. Haldane, “Fractional quantization of the Hall effect: a hierarchy of incompressible quantum fluid states,” *Phys. Rev. Lett.* **51**, p. 605, 1983.
- [50] B. I. Halperin, “Statistics of quasiparticles and the hierarchy of fractional quantized Hall states,” *Phys. Rev. Lett.* **52**, p. 1583, 1984.
- [51] B. I. Halperin, “Theory of the quantized Hall conductance,” *Helv. Phys. Acta* **56**, p. 75, 1983.
- [52] R. E. Prange and S. M. Girvin, *The Quantum Hall Effect*, Springer Verlag, New York, 1990.
- [53] P. Sitko, K.-S. Yi, and J. J. Quinn, “Composite fermion hierarchy: Condensed states of composite fermion excitations,” *Phys. Rev. B* **56**, pp. 12417–12421, 1997.
- [54] S. Das Sarma and A. Pinczuk, *Perspectives in Quantum Hall Effects: Novel Quantum Liquids in Low-Dimensional Semiconductor Structures*, Wiley, New York, 1997.
- [55] F. Wilczek, *Fractional Statistics and Anyon Superconductivity*, World Scientific, Singapore, 1990.
- [56] R. L. Willett, “The quantum Hall effect at $5/2$ filling factor,” *Rep. Prog. Phys.* **76**, p. 076501, 2013.
- [57] J. S. Birman, *Braids, Links and Mapping Class Groups*, Princeton UP, Princeton, 1974.
- [58] E. Spanier, *Algebraic topology*, Springer-Verlag, Berlin, 1966.
- [59] T. Einarsson, “Fractional statistics on a torus,” *Phys. Rev. Lett.* **64**, p. 1995, 1990.
- [60] Y. S. Wu, “General theory for quantum statistics in two dimensions,” *Phys. Rev. Lett.* **52**, p. 2103, 1984.
- [61] J. M. Leinaas and J. Myrheim, “On the theory of identical particles,” *Nuovo Cimento* **37B**, p. 1, 1977.

- [62] E. C. G. Sudarshan, T. D. Imbo, and T. R. Govindarajan, “Configuration space topology and quantum internal symmetries,” *Phys. Lett. B* **213**, p. 471, 1988.
- [63] T. D. Imbo, C. S. Imbo, and C. S. Sudarshan, “Identical particles, exotic statistics and braid groups,” *Phys. Lett. B* **234**, p. 103, 1990.
- [64] M. G. Laidlaw and C. M. DeWitt, “Feynman functional integrals for systems of indistinguishable particles,” *Phys. Rev. D* **3**, p. 1375, 1971.
- [65] R. P. Feynman and A. R. Hibbs, *Quantum Mechanics and Path Integrals*, McGraw-Hill, New York, 1964.
- [66] M. Chaichian and A. Demichev, *Path Integrals in Physics, Volume I and II*, IOP Publishing Ltd, Bristol; Philadelphia, 2001.
- [67] M. Azbel, “Energy spectrum of a conduction electron in a magnetic field,” *J. Exp. Theor. Phys.* **19**, p. 634, 1964.
- [68] D. R. Hofstadter, “Energy levels and wave functions of Bloch electrons in rational and irrational magnetic fields,” *Phys. Rev. B* **14**, p. 2239, 1976.
- [69] O. Ciftja and C. Wexler, “Monte Carlo simulation method for Laughlin-like states in a disk geometry,” *Phys. Rev. B* **67**, p. 075304, 2003.
- [70] N. Metropolis, A. W. Rosenbluth, M. N. Rosenbluth, A. M. Teller, and E. Teller, “Equation of state calculations by fast computing machines,” *J. Chem. Phys.* **21**, p. 1087, 1953.
- [71] W. Pan, K. W. Baldwin, K. W. West, L. N. Pfeiffer, and D. C. Tsui, “Fractional quantum Hall effect at Landau level filling $4/11$,” *Phys. Rev. B* **91**, p. 041301(R), 2015.
- [72] S. Mukherjee, S. S. Mandal, Y. Wu, A. Wójs, and J. K. Jain, “Enigmatic $4/11$ state: A prototype for unconventional fractional quantum hall effect,” *Phys. Rev. Lett.* **112**, p. 016801, 2014.
- [73] A. A. Abrikosov, L. P. Gorkov, and I. E. Dzyaloshinskii, *Methods of Quantum Field Theory in Statistical Physics*, Dover Publ. Inc., Dover, 1975.
- [74] X. Du, I. Skachko, F. Duerr, A. Luican, and E. Y. Andrei, “Fractional quantum Hall effect and insulating phase of Dirac electrons in graphene,” *Nature* **462**, p. 192, 2009.
- [75] L. Romasanta, M. Hernandez, M. Lopez-Manchado, and R. Verdejo, “Functionalised graphene sheets as effective high dielectric constant fillers,” *Nanoscale Research Letters* **6**, p. 508, 2011.
- [76] M. O. Goerbig, “Electronic properties of graphene in a strong magnetic field,” *Rev. Mod. Phys.* **83**, p. 1193, 2011.
- [77] E. McCann and M. Koshino, “The electronic properties of bilayer graphene,” *Rep. Prog. Phys.* **76**, p. 056503, 2013.
- [78] B. E. Feldman, A. J. Levin, B. Krauss, D. A. Abanin, B. I. Halperin, J. H. Smet, and A. Yacoby, “Fractional quantum Hall phase transitions and four-flux states in graphene,” *Phys. Rev. Lett.* **111**, p. 076802, 2013.
- [79] P. Maher, L. Wang, Y. Gao, C. Forsythe, T. Taniguchi, L. Watanabe, D. Abanin, Z. Papić, P. Cadden-Zimansk, J. Hone, P. Kim, and C. R. Dean, “Tunable fractional quantum Hall phases in bilayer graphene,” *Science* **345**, p. 61, 2014.
- [80] M. Z. Hasan and C. L. Kane, “Colloquium: Topological insulators,” *Rev. Mod. Phys.* **82**(3045), 2010.
- [81] R. D. Wiersma, J. G. S. Lok, S. Kraus, W. Dietsche, K. von Klitzing, D. Schuh, M. Bichler, H. P. Tranitz, and W. Wegscheider, “Activated transport in the separate layers that form the $\nu_T = 1$ exciton condensate,” *Phys. Rev. Lett.* **93**, p. 266805, 2004.
- [82] J. I. A. Li, T. Taniguchi, K. Watanabe, J. Hone, and C. R. Dean, “Excitonic superfluid phase in double bilayer graphene,” *Nat. Phys.* **13**, p. 751, 2017.
- [83] X. Liu, K. Watanabe, T. Taniguchi, B. I. Halperin, and P. Kim, “Quantum Hall drag of exciton condensate in graphene,” *Nat. Phys.* **13**, p. 746, 2017.
- [84] J. Eisenstein, “Evidence for spontaneous interlayer phase coherence in a bilayer quantum Hall exciton condensate,” *Sol. St. Comm.* **127**, p. 123, 2003.
- [85] H. A. Fertig, “Energy spectrum of a layered system in a strong magnetic field,” *Phys. Rev. B* **40**, p. 1087, 1989.
- [86] L. P. Gorkov and I. E. Dzyaloshinskii, “Contribution to the theory of the Mott exciton in a strong magnetic field,” *Sov. Phys. JETP* **26**, p. 449, 1968.
- [87] E. Tutuc and M. Shayegan, “Charge neutral counterflow transport at filling factor 1 in GaAs hole bilayers,” *Sol. St. Comm.* **144**, p. 405, 2007.

- [88] Y. W. Suen, L. W. Engel, M. B. Santos, M. Shayegan, and D. C. Tsui, "Observation of a $\nu=1/2$ fractional quantum hall state in a double-layer electron system," *Phys. Rev. Lett.* **68**, p. 1379, 1992.
- [89] P. Eisenstein, G. S. Boebinger, L. N. Pfeiffer, K. W. West, , and S. He, "New fractional quantum Hall state in double-layer two-dimensional electron systems," *Phys. Rev. Lett.* **68**, p. 1383, 1992.

5. Elaboration of remaining publications of the author after PhD

- Publications after PhD concerning the habilitation achievement not included to the dissertation

1. **J. Jacak**, P. Łydźba, and L. Jacak, *Homotopy approach to fractional quantum Hall effect*. Appl. Math. 6, p. 345, 2015.
2. **J. Jacak** and L. Jacak, *The triggering role of carrier mobility in the fractional quantum Hall effect formation—an evidence in graphene*. J. Mod. Phys. 4, p. 1591, 2013. invited to Special Issue: Topological Insulators and Low Dimensional Quantum Physics.
3. **J. Jacak**, P. Łydźba, and L. Jacak, *Fractional quantum Hall effect revisited*. Physica B 475, p. 122, 2015.
4. **J. Jacak**, *Bilayer graphene as the material for study of the unconventional fractional quantum Hall effect*. chapter in Graphene Materials: Structure, Properties and Modifications, G. Z. Kyzas, ed., ch. 3, pp. 49–76, INTECH, 2017.
5. **J. Jacak**, R. Gonczarek, L. Jacak, and I. Józwiak, *Explanation of composite fermion structure in fractional quantum Hall systems*. Int. J. Mod. Phys. B 26, pp. 1230011–1–60, 2012.
6. P. Łydźba and **J. Jacak**, *Ultra-quantum 2d materials: Graphene, bilayer graphene, and other Hall systems—new non-local quantum theory of Hall physics*. chapter in Recent Advances in Graphene Research, P. Nayak, ed., ch. 1, pp. 3–29, INTECH, 2016.
7. **J. Jacak**, 2017, *Confinement and fractional charge of quarks from braid group approach to holographic principle*, arXiv:1704.06560.
8. **J. Jacak**, L. Jacak, 2015, *Hierarchy of fillings for FQHE in monolayer and in bilayer graphene: Explanation of $\nu = -\frac{1}{2}$ fractional quantum Hall state in bilayer graphene*, arXiv:1503.08783.
9. **J. Jacak**, L. Jacak, 2014, *Explanation of the odd structure of fractional Hall states in higher Landau levels and filling ratios with even denominators*, arXiv:1405.4348.
10. **J. Jacak**, L. Jacak, 2014, *Explanation of fractional hierarchy observed experimentally in higher Landau levels*, arXiv:1405.2598.
11. **J. Jacak**, L. Jacak, 2012, *Confirmation in graphene of wave packet multilooped dynamics related to fractional quantum Hall state*, arXiv:1201.4452.
12. **J. Jacak**, L. Jacak, 2012, *The triggering role of carrier mobility in the fractional quantum Hall effect-evidence in graphene*, arXiv:1201.4451.

- Publications after PhD not concerning the topic of the habilitation achievement

13. M. Jacak, I. Józwiak, **J. Jacak**, J. Gruber, W. Jacak, 2013, *Wprowadzenie do kryptografii kwantowej: implementacja protokołów kryptografii kwantowej na systemach niesplątanych fotonów (system Clavis II) i splątanych fotonów (system EPR S405 Quelle) (Introduction to quantum cryptography: implementations of QC protocols on non-entangled system Clavis II and on entangled photon system EPR S405 Quelle)*, ISBN: 978-83-7493-746-7, PWR Edition, Wrocław 2013, monograph, 1-200.
14. M. Jacak, **J. Jacak**, I. Józwiak, P. Józwiak, 2016, *Quantum cryptography: Theoretical protocols for quantum key distribution and tests of selected commercial QKD systems in commercial fiber networks*, International Journal of Quantum Information **14**, 1630002-1-73.

15. M. Jacak, D. Melniczuk, **J. Jacak**, A. Janutka, I. Jóźwiak, J. Gruber, P. Jóźwiak, 2016, *Quantum key distribution security constraints caused by controlled quality of dark channel for non-entangled and entangled photon quantum cryptography setups*, *Optical and Quantum Electronics* **48**, 363-1-16.
 16. M. Jacak, D. Melniczuk, **J. Jacak**, I. Jóźwiak, J. Gruber, P. Jóźwiak, 2015, *Stability assessment of QKD procedures in commercial quantum cryptography systems versus quality of dark channel*, *International Journal of Quantum Information* **13**, 1550064-1-12.
 17. E. Zielony, E. Płaczek-Popko, A. Henrykowski, Z. Gumienny, P. Kamyczek, **J. Jacak**, P. Nowakowski, G. Karczewski, 2012, *Laser irradiation effects on the CdTe/ZnTe quantum dot structure studied by Raman and AFM spectroscopy*, *International Journal of Applied Physics* **112**, 063520-1-7.
- Publications accepted – in press (at 31.07.2018)
 18. **J. Jacak**, 2018, *Topological approach to Fractional Quantum Hall Effect in monolayer and bilayer graphene*, *Handbook on the Graphene Materials (Advanced Materials Book Series)*, VBRI Press, Wiley, invited chapter.
 19. P. Łydźba, **J. Jacak**, 2018, *Many-body wave functions for correlated systems in magnetic fields: Monte Carlo simulations in the lowest Landau level*, *Journal of Physics: Cond. Matter*,
 20. **J. Jacak**, W. Jacak, 2018, *Plasmon-induced enhancement of efficiency of solar cells modified by metallic nano-particles: material dependence*, *Journal of Applied Physics*.
 - Patents (submitted)
 21. Patent Polish and European, **J. Jacak**, W. Jacak, W. Donderowicz, L. Jacak, *Entanglement Quantum Random Number Generator with public randomness certification*, 2017/2018
 22. Patent Polish and European, **J. Jacak**, W. Jacak, *The One-Qubit Pad (OQP) for entanglement encryption of quantum information*, 2017/2018
 23. Patent Polish, W. Jacak, **J. Jacak**, W. Donderowicz, L. Jacak, *Kwantowa Splątaniowa Waluta - Quantum Entanglement Currency (QEC)*, 2017
 24. Patent Polish, M. Jacak, **J. Jacak**, W. Jacak, W. Donderowicz, L. Jacak, *BANQOMAT - zabezpieczony kryptografią kwantową bankomat – Quantum cryptography protected ATM*, 2017
 25. Patent Polish, **J. Jacak**, W. Jacak, W. Donderowicz, L. Jacak, *Kwantowy Splątaniowy Podpis Cyfrowy - Quantum Entanglement Digital Signature (QEDS)*, 2017

Publications of J. Jacak after PhD not included to the habilitation dissertation but concerning the topic of the dissertation are – 12 publications listed above. Moreover J. Jacak is the coauthor of 5 publications after his PhD from other field – mostly of quantum information processing, and also 5 patents (submitted) from quantum information and quantum cryptography domain and recently, of plasmonics, moreover, 3 other publications are in press (at 31.07.2018).

The publications in the topic of habilitation dissertation not included to the presented in the point 4. a), b) scientific achievement are supplementary to publications listed in the point 4. b). According to the list above, the publications 2,4,6 are review chapters in books (monographs or special issue) (including invited chapters). There are presented there the main aspects of the developed by the author new topological formulation of the FQHE theory and its applications mostly in graphene. The publications 1,3,5 are also of

summarizing character or describe some details from the papers included to the habilitation achievement. In particular, an extensive (60 pages) publication 5 is correlated with the monograph in World Scientific (J. Jacak, R. Gonczarek, L. Jacak, and I. Józwiak, Application of Braid Groups in 2D Hall System Physics: *Composite Fermion Structure*, World Scientific, Singapore, 2012) but contains some new elements developed further in next author publications. The publications 1 – 12 contain also miscellaneous particular results not published in the cycle listed in the point 4. b) – they are of some supplementary character to the whole achievement. Publications 7 – 12 are arXivs, in majority published next in regular journals. An exception is the paper 7 concerning a novel proposition of the author of application of braid group method to an original concept of quarks as anyons on a holographic sphere-like-boundary toward contribution to the problem of quark confinement in hadrons and of their fractional charge – submitted to publication in journal.

The next group of publications of the author after PhD is related with a different field – mostly quantum cryptography. To this group belong: 13 – the monograph (TU Ed.) in the field of quantum cryptography and quantum key distribution (toward practical implementations of quantum cryptography on entangled and non-entangled photons), and three next publications (14 – 16 according to the list above) concerning development of practical implementations of quantum key distribution (QKD). These papers resulted from collaboration of the author with the group from Austrian Institute of Technology (spin-off University in Vienna, linked with prof. Zeilinger group) in the range of the implementation of QKD on entangled photons and with the commercial company in QKD, idQuantique from Geneva (spin-off University in Geneva, linked with group of prof. Gisin) in the range of QKD employing non-entangled photons, with regard to application of both systems in metropolitan fiber network in Wrocław and laboratory tests of various versions of quantum dark channel, as well as of development of own construction of QKD system. With the latter are linked also 5 patents submissions (Polish and European) (21 – 25 according to the list above) concerning the development and application of QKD and of novel constructions of quantum generator of random numbers. The submitted patents 21 – 25 (2017/2018) are results of collaboration of J. Jacak upon the projects in quantum information processing and information security with the team from Department of Quantum Technologies WUST.

The paper 17 concerns the Raman spectroscopy – J. Jacak took course (of two week long carried by French producer) of Raman spectroscopy (on the spectrometer T64000 Horiba-J-Y) and participated in related experimental research resulted in publication 17.

Moreover, there are supplementarily listed 3 papers, 18,19,20, at the moment (31.07.2018) accepted in journals and being in press. The position 18 is the invited review chapter on topological approach to FQHE in graphene to a specialist monograph by Wiley. The paper 19 presents the numerical illustration (by Metropolis Monte-Carlo simulation) of the author approach to the FQHE in the LLL of conventional GaAs Hall system. The paper 20 concerns the application of plasmonics to enhance efficiency of solar cells metallicly modified in nano-scale – this contribution is targeted for participation of WUST group in EU project, COST action MiltiscaleSolar in continuation of former author activity in plasmonics in collaboration with prof. J. Karsnyj (Odessa University) and prof. D. Schaadt (Karlsruhe/Clausthal University).

